PL-TR-97-2044 MFD-FR-97-15727

The Physical Basis for the Lg/P Discriminant: General Properties and Preliminary Modeling

Theron J. Bennett
Keith L. McLaughlin
Margaret E. Marshall
Jeffry L. Stevens

Maxwell Technologies, Inc.
8888 Balboa Ave.
San Diego, CA 92123-1506

March, 1997

Scientific Report No. 1

Approved for public release; distribution unlimited

PHILLIPS LABORATORY
Directorate of Geophysics
AIR FORCE MATERIEL COMMAND
HANSCOM AIR FORCE BASE, MA 01731-3010

SPONSORED BY
Air Force Technical Applications Center
Directorate of Nuclear Treaty Monitoring
Project Authorization T/5101

MONITORED BY
Phillips Laboratory
CONTRACT No. F19628-95-C-0107

The views and conclusions contained in this document are those of the authors and should not be interpreted as representing the official policies, either express or implied, of the Air Force or U.S. Government.

This technical report has been reviewed and is approved for publication.

Delaine Reiter

DELAINE R. REITER
Contract Manager
Earth Sciences Division

James F. Lewkowicz

JAMES F. LEWKOWICZ
Director
Earth Sciences Division

This report has been reviewed by the ESD Public Affairs Office (PA) and is releasable to the National Technical Information Service (NTIS).

Qualifed requestors may obtain copies from the Defense Technical Information Center. All others should apply to the National Technical Information Service.

If your address has changed, or you wish to be removed from the mailing list, or if the addressee is no longer employed by your organization, please notify PL/IM, 29 Randolph Road, Hanscom AFB, MA 01731-3010. This will assist us in maintaining a current mailing list.

Do not return copies of this report unless contractual obligations or notices on a specific document requires that it be returned.

REPORT DOCUMENTATION PAGE

Form Approved
OMB No. 0704-0188

1. AGENCY USE ONLY *(Leave blank)*	2. REPORT DATE	3. REPORT TYPE AND DATES COVERED
	March, 1997	Scientific No.1

4. TITLE AND SUBTITLE

THE PHYSICAL BASIS FOR THE L_g/P DISCRIMINANT: GENERAL PROPERTIES AND PRELIMINARY MODELING

5. FUNDING NUMBERS

Contract No.
F19628-95-C-0107

PE 35999F

PR 5101 TA GM

WU AG

6. AUTHOR(S)

Theron J. Bennett, Keith L. McLaughlin, Margaret E. Marshall, and Jeffry L. Stevens

7. PERFORMING ORGANIZATION NAME(S) AND ADDRESS(ES)

Maxwell Technologies, Inc.
8888 Balboa Avenue
San Diego, CA 92123-1514

8. PERFORMING ORGANIZATION REPORT NUMBER

MFD-FR-97-15727

9. SPONSORING/MONITORING AGENCY NAME(S) AND ADDRESS(ES)

Phillips Laboratory
29 Randolph Road
Hanscom AFB, MA 01731-3010

Contract Manager: James C. Battis/VSBI

10. SPONSORING/MONITORING AGENCY REPORT NUMBER

PL-TR-97-2044

11. SUPPLEMENTARY NOTES

12a. DISTRIBUTION/AVAILABILITY STATEMENT

Approved for public release; distribution unlimited

12b. DISTRIBUTION CODE

13. ABSTRACT *(Maximum 200 words)*

A critical problem for reliable implementation of regional discrimination is incomplete understanding of how regional seismic signals depend on physical characteristics of the source and propagation path to the recording station. This research is directed at improving understanding of effects of these characteristics on an important regional discriminant, the L_g/P ratio. An empirical element in this research program has aimed at describing behavior of L_g/P ratios and their dependence on frequency for nuclear explosions, earthquakes, rockbursts, and other sources in various tectonic environments. Observations indicate differences between event types which appear to be enhanced at higher frequencies, but sources of scatter in the observations need further study. The theoretical element of this project seeks to explain the main features of the L_g/P observations in terms of source mechanisms and propagation models for the regional signals. Initial focus of the theoretical studies has been on effectiveness of mechanisms for generation of L_g by explosive sources. The studies indicate that, even though R_g-to-L_g scattering might explain observed frequency dependence and other features of explosion L_g/P ratios, it probably provides only a minor contribution to explosion Lg signals compared to other mechanisms.

14. SUBJECT TERMS

Seismic	Regional	Spectra	Source
Discrimination	L_g/P	Mechanism	Propagation

15. NUMBER OF PAGES 56

16. PRICE CODE

17. SECURITY CLASSIFICATION OF REPORT	18. SECURITY CLASSIFICATION OF THIS PAGE	19. SECURITY CLASSIFICATION OF ABSTRACT	20. LIMITATION OF ABSTRACT
UNCLASSIFIED	UNCLASSIFIED	UNCLASSIFIED	UNLIMITED

Table of Contents

Page

List of Illustrations

List of Tables

1. Introduction

1.1 Objectives

The Comprehensive Test Ban Treaty (CTBT) will require the detection and identification of seismic events down to low magnitudes. This requirement will make it necessary to rely on regional seismic monitoring to locate and identify small events. Although considerable progress has been made over the past decade in understanding the characteristics of regional seismic signals, effective regional discriminants, which can be applied generally, have yet to be determined. The two fundamental problems which remain for regional discrimination are (1) lack of adequate empirical data from different source types and different regions to provide the necessary calibration of regional discrimination techniques, and (2) incomplete understanding of how regional seismic signals depend on physical characteristics of the source and on the propagation environment along the path to the recording station. The goal of this research project is to improve physical understanding of the effects of source and propagation on a specific regional discriminants - viz. the L_g/P ratio. Over the years, the L_g/P ratio has proven to be one of the more promising and enduring measures for distinguishing between explosions and earthquakes. By improving understanding of the physical basis for this discriminant, we hope to acquire the knowledge which will enable more reliable application of the discriminant and the extension of regional discrimination capabilities into uncalibrated regions.

To reach this objective, the research program includes an empirical element aimed at determining the characteristic behavior of L_g/P ratios and their dependence on frequency and distance for the various source types of interest and for different source regions where these observations are available. These empirical observations are then used to constrain theoretical models representing the source types and regional propagation paths. The models which are derived and refined from this process can be used to improve understanding of the physical basis for discriminating events with L_g/P ratios.

1.2 Accomplishments

For use in the empirical element of this research program, we have collected regional waveform data from a variety of source types including nuclear explosions, earthquakes, rockbursts, and chemical blasts for a range of propagation environments. Most regional waveform data for nuclear tests are available from only a few source regions (viz. the Nevada Test Site (NTS) in the United States, the former Soviet test sites at Shagan River (SR) in East Kazakhstan and at Novaya Zemlya (NZ), and the Chinese test site at Lop Nor). To provide a wider range of source and propagation environments, we have sought to supplement the nuclear explosion database with data from additional underground nuclear explosions which were conducted in many areas of the former Soviet Union as part of the Peaceful Nuclear Explosion (PNE) program. For comparison to other source types, we have collected regional data from seismic sources other than nuclear explosions in the same or nearby regions. These data include mainly earthquakes near NTS and elsewhere in the western U.S., earthquakes along the southern border of the former Soviet Union and farther south into China and other neighboring countries, and earthquakes in Europe, Scandinavia, and several other regions. Records from some non-nuclear explosions in a few different source areas are also in the database. In addition, we have included regional seismic data from rockbursts and other mining-induced events from many different regions, such as South Africa, Central Europe, and the eastern and western U.S. We are continuing to supplement the database with more recent events of all types recorded at the modern IDC and other digital stations for areas of interest.

In analyzing the seismic waveform data from these events, we have used both Fourier spectral analyses and band-pass filter analyses of the signals at regional stations to determine amplitudes in group-velocity windows corresponding to L_g and regional P. Ratios between regional phases (viz. L_g/P) at spectral frequencies or at filter center frequencies have been determined; and the spectral ratios were plotted as a function of frequency. We are still experimenting somewhat to determine the most effective ways to measure these regional phase spectra and spectral ratios. Alternative group velocity windows, frequency bands, and amplitude averaging techniques are being assessed. We are also investigating effects of source region and attenuation on L_g/P ratios.

Results from our initial investigations are generally in agreement with past findings which indicate that L_g/P ratios are lower for nuclear explosions than for other types of sources with the largest differences observed at higher frequencies. The ratios for rockbursts and earthquakes tend to be similar, showing relatively high values (near one) over a fairly broad range of high frequencies; while the ratios for nuclear explosions normally fall well below one at high frequencies. Some of our best-controlled observations are from nearer-regional stations surrounding NTS explosions and nearby earthquakes, while our experience from Eurasian explosions and earthquakes generally involves more-distant regional stations. Our results show differences in the L_g/P ratio behavior with frequency for the same source types from the different sets of observations. The ratios generally show less rapid decline with increasing frequency for NTS explosions than for East Kazakhstan explosions. We have been attempting to determine whether this effect can be explained by attenuation differences or whether source excitation differences might also be a factor.

With regard to theoretical modeling of the behavior of the L_g and regional P signals from different types of seismic sources, a long-standing problem has been to adequately explain the S or L_g signals associated with nuclear explosions. Several possible mechanisms for generation of such signals are under consideration; these mechanisms generally can be grouped into two categories: (1) those related to indirect conversion of energy radiated by the isotropic explosion source into S waves, or (2) non-isotropic components added to the explosion to produce a composite source which generates the S waves. We have been attempting to evaluate the effectiveness of several such mechanisms for L_g generation within some representative crustal models. The crustal models which we have used in these analyses so far include a Gutenberg earth model, along with models for NTS and for the former Soviet test site in East Kazakhstan. One mechanism for L_g generation from the explosion source which has been analyzed is $R_g \rightarrow L_g$ scattering. Our initial model studies suggest that this mechanism can possibly explain some of the observed characteristics of regional signals from buried nuclear explosion sources, but maybe not others. In particular, the model predicts that $R_g \rightarrow L_g$ scattering for frequencies near 1 Hz is probably as effective as near-source $P \rightarrow S$ conversions at horizontal interfaces. However, this mechanism may not be capable of producing the relatively large L_g/P ratios observed from nuclear explosions at frequencies of 1 Hz and lower; and at higher frequencies this mechanism for L_g generation is quite ineffective. Additional studies of this and other mechanisms for producing the observed behavior of L_g/P ratios with frequency for explosion sources are currently being pursued. We will ultimately seek to explain the different effects of the explosion and non-explosion mechanisms on this behavior for representative crustal models.

1.3 Report Organization

This report is divided into five sections including these introductory remarks. Section 2 describes the event database which we have been working with. Section 3 discusses the results from the analyses of the empirical data in several different regions. Section 4 describes the modeling studies which have been performed, focusing on investigations of the physical mechanism and efficiency of generation of L_g signals by explosion sources. Section 5 summarizes the preliminary results and describes the plan for continuing work to determine the physical basis for the L_g/P regional discriminant.

2. Database for Regional Discrimination

2.1 Availability of Regional Data for Discrimination Studies

Regional recordings of underground nuclear explosions cover a very limited domain in space and time. Over the years the most active test sites have been at NTS in the western U.S., near Shagan River in East Kazakhstan, and Novaya Zemlya in the Russian arctic. In addition, numerous tests were conducted by the former Soviet Union in the North Caspian basin and elsewhere throughout their former territories as part of the Peaceful Nuclear Explosions (PNE) program. France has also detonated numerous nuclear explosions at a site in the South Pacific and, prior to that, in northern Africa. Additional nuclear explosion tests have been conducted in western China at Lop Nor, and there have been scattered events in other source regions. So, while there have been underground nuclear explosions in a variety of geographic areas around the world, there are large portions of the world where there is little or no experience with nuclear tests. In comparison, earthquakes and other seismic sources also occur in many regions throughout the world; but the areas around many of the nuclear explosion test sites are relatively inactive with respect to these alternate sources. As a result, direct empirical comparisons may not be convincing unless a proper physical understanding can be developed to serve as the basis for analyzing regional signals from different source types and propagation regions.

A second factor affecting availability of data for regional discrimination studies is the history of seismic monitoring. The seismic monitoring environment is continually changing as newer, better-quality single stations and arrays are fielded and calibrated. However, because of testing moratoria and the tapering off of the nuclear testing programs in most countries, there are little or no data available from nuclear explosions at many of the more modern stations. The new data alone are inadequate to calibrate regional discrimination capabilities, particularly at the level which would be required for reliable CTBT monitoring. The historical regional data can be useful in helping to infer the characteristics of regional signals from potential nuclear tests in uncalibrated regions. A physical basis for such inferences is critical to understanding the behavior of discriminant measures and how they are likely to perform in such regions. After establishing the physical basis for regional discrimination, the regional observations for alternative event types from the modern station network can be reassessed to evaluate CTBT event identification capabilities.

2.2 Event and Station Locations from Historical Database

In a previous report (cf. Bennett et al., 1996), we described the characteristics of the regional seismic database of underground nuclear explosions and earthquakes which we have been working with to improve discrimination capability. We also discussed there what additional data from some of these historical seismic stations might be available and useful for supplementing the current database. In this report we will only summarize the database description from our previous study. Traditionally, the best controlled data sample for analyzing the differences between regional signals from nuclear explosions and earthquakes is the large body of regional recordings from NTS nuclear explosions and nearby earthquakes (cf. Murphy and Bennett, 1982; Bennett and Murphy, 1986; Taylor et al., 1989). In the course of our regional discrimination studies over the years, we have collected digital waveform data from selected NTS nuclear explosions and earthquakes in the surrounding regions. In general, we have tried to select earthquakes and explosions for direct comparison which have similar propagation paths, so that attenuation differences would not be a significant factor. As a result, the majority of earthquakes in the database are events with epicenters within about 100 km of NTS. The majority of these earthquakes tend to be small. To provide comparisons at some of the more distant stations, we have relaxed this constraint somewhat and included larger explosions and earthquakes with somewhat greater source separation but still with roughly comparable epicentral distances, and thus similar propagation. Figure 1 shows the locations of the stations in this database for western U.S. events. Much of the data comes from nearer-regional stations; signal-to-noise levels tend to be poor at the farther stations, especially for L_g, although regional signals are strong in some frequency bands for larger events even at far-regional stations. The map in Figure 2 shows the locations of stations in Eurasia from which we have collected good regional signals from Eurasian

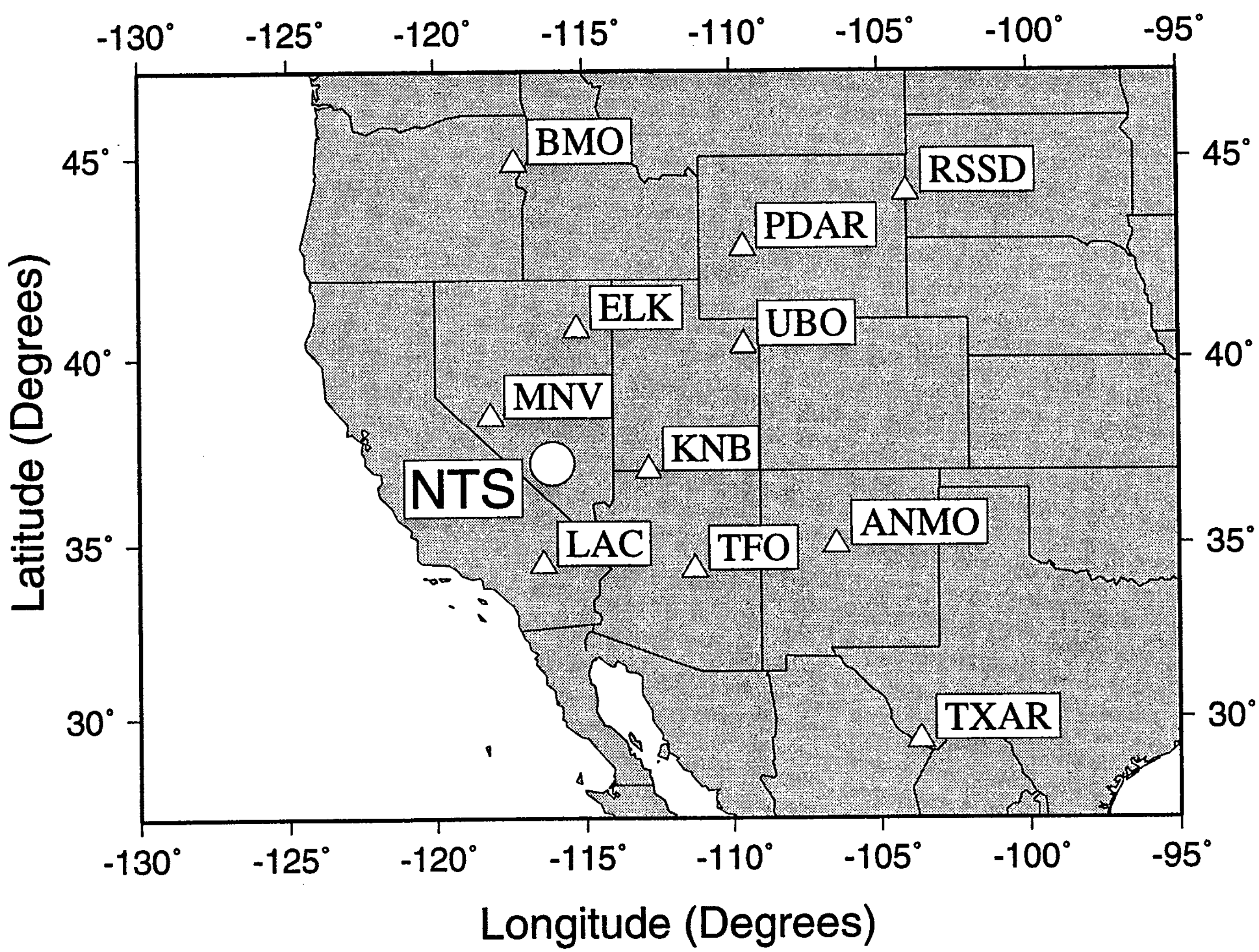

Figure 1. Map of western U.S. showing location of NTS relative to regional stations with good digital data which are currently in the database.

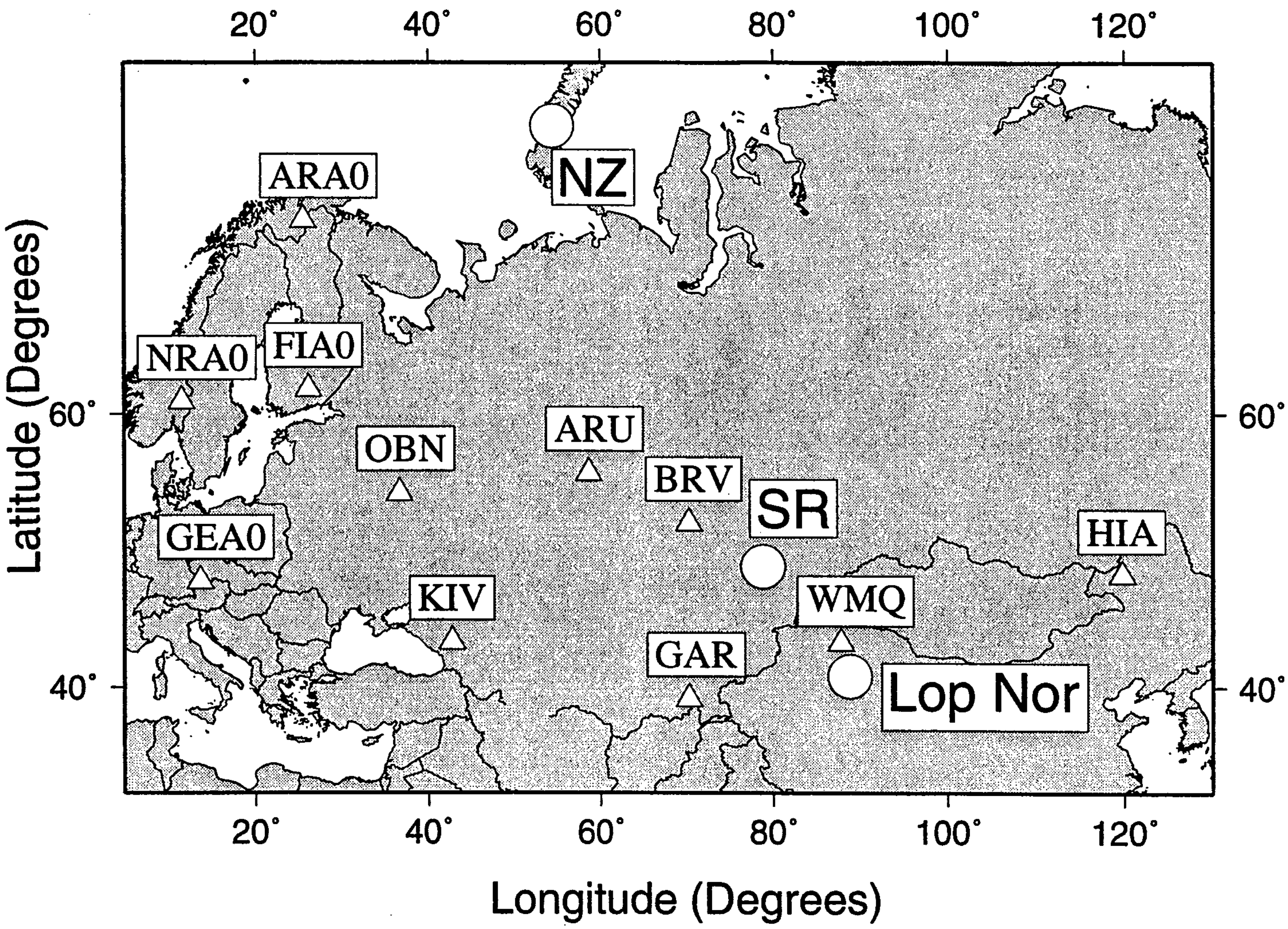

Figure 2. Map of Eurasia showing location of principal nuclear test sites relative to regional stations with good digital data which are currently in the database.

nuclear explosions and earthquakes in the current database. In this case, many of the data come from farther regional stations; the signal-to-noise levels tend to be fairly high on broadband records for many of the larger magnitude events, although the S and L_g signals sometimes have limited useful bandwidth at these greater distances.

Figures 3 through 6 summarize the distribution of the observations in our regional database with respect to epicentral distance and event magnitude. In this presentation we have combined the samples from the western U.S. and Eurasia; in our prior report (cf. Bennett et al., 1996) we provided separate distributions for these regions and compared between the regions. Figures 3 and 4 show the distributions with respect to epicentral distance for nuclear explosions and earthquakes, respectively. The distributions appear similar with the data concentrated at ranges less than 1000 km for both source types. This is primarily due to the prevalence of nearer-regional stations in the western U.S. database for nuclear explosions. It is noteworthy in this regard that, in assembling the database, we deliberately sought nearby events of similar magnitudes for comparison; and, because most earthquakes occurring near NTS were small, we also sought small explosions which were not necessarily very well recorded at more distant stations. In contrast, the regional data from Eurasian seismic events tend to be concentrated at distance ranges of 1000 km and beyond. This is primarily because the seismic stations available for recording nuclear explosions from the former Soviet Union were generally located at far-regional distances from the principal test sites, and again we sought earthquake observations for comparison which would be at similar epicentral distances.

Figures 5 and 6 show the distributions of the regional data in the database with respect to magnitude for nuclear explosions and earthquakes respectively. The distributions are somewhat similar, although the earthquake distribution tends to be spread over a broader magnitude range and appears to be biased somewhat toward slightly lower magnitudes than the nuclear explosions. This is related to the difficulty alluded to above in trying to find large earthquakes in proximity to the nuclear test sites for use in comparisons. It should be noted, with regard to the L_g/P ratio discriminant, that such magnitude differences are probably less critical than for the L_g spectral ratio

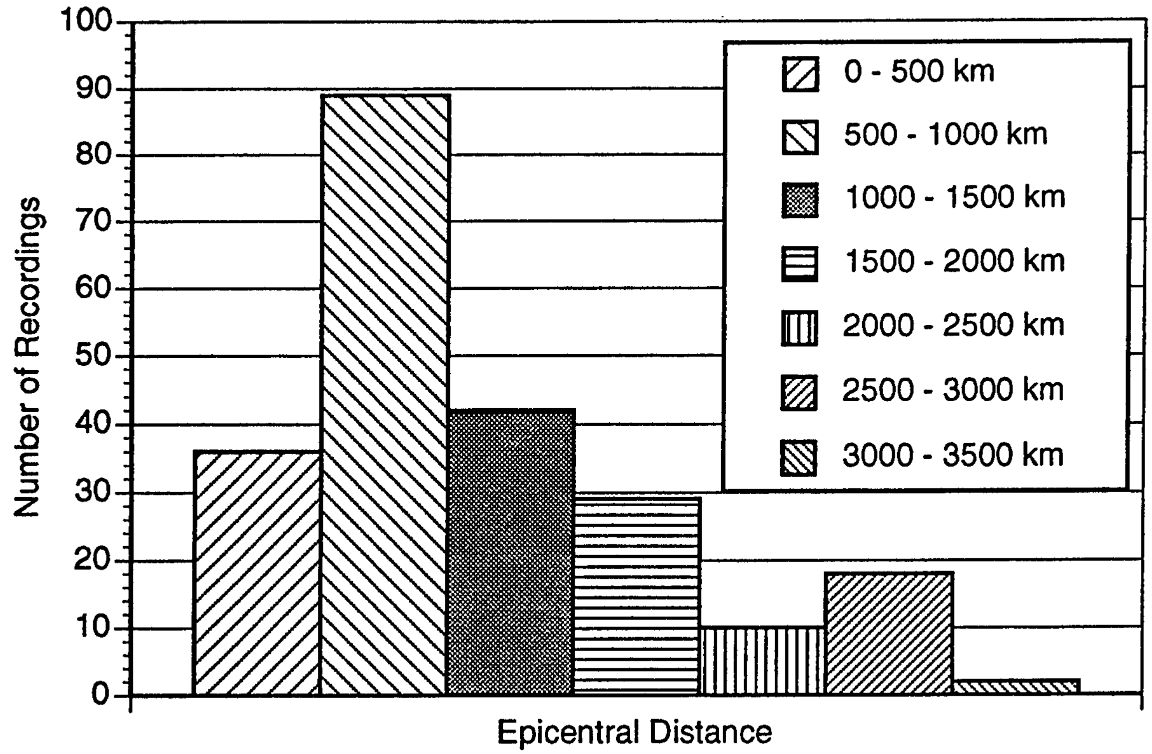

Figure 3. Distribution of observations for selected nuclear explosions in western U.S. and Eurasia providing good regional signals in the current database.

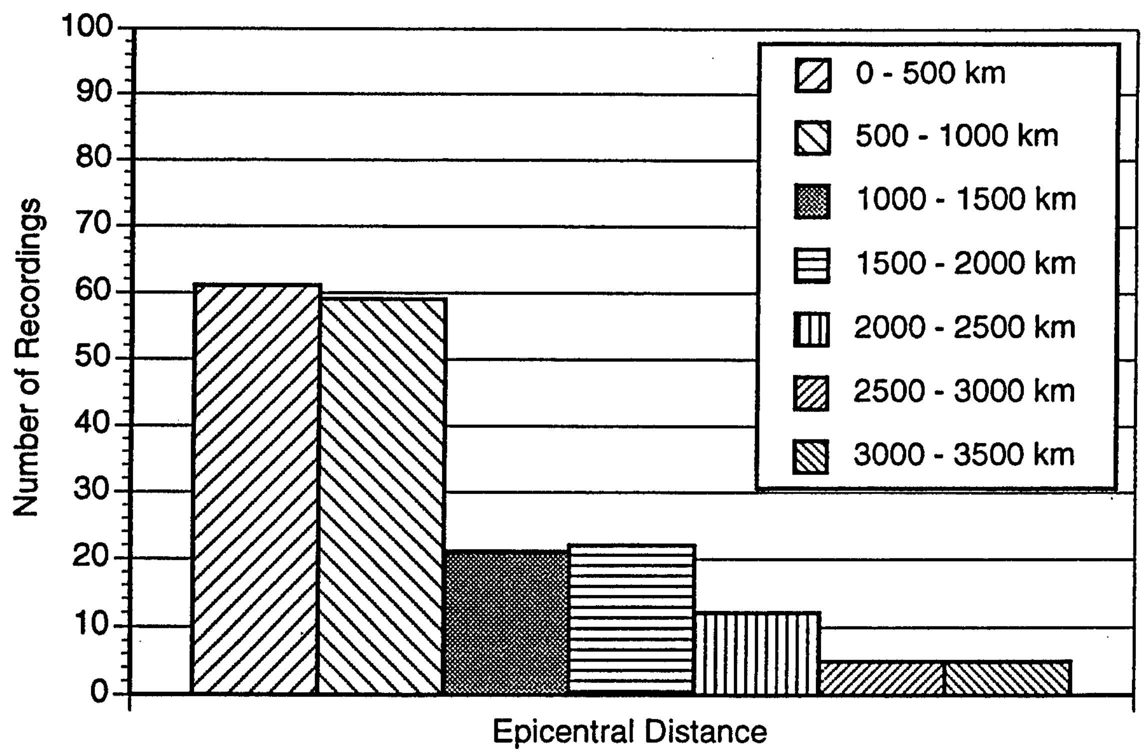

Figure 4. Distribution with respect to distance of observations for selected earthqyakes in western U.S. and Eurasia providing good regional signals in the current database.

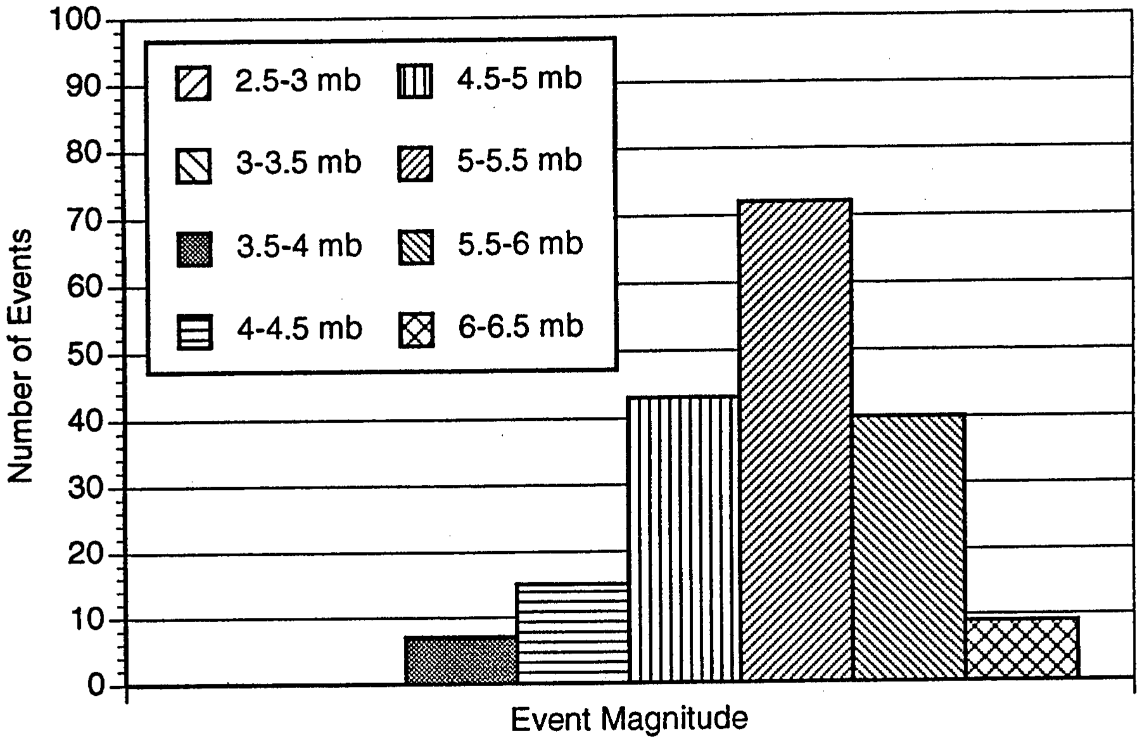

Figure 5. Distribution with respect to magnitude of observations for nuclear explosions in the western U.S. and Eurasia in the current database.

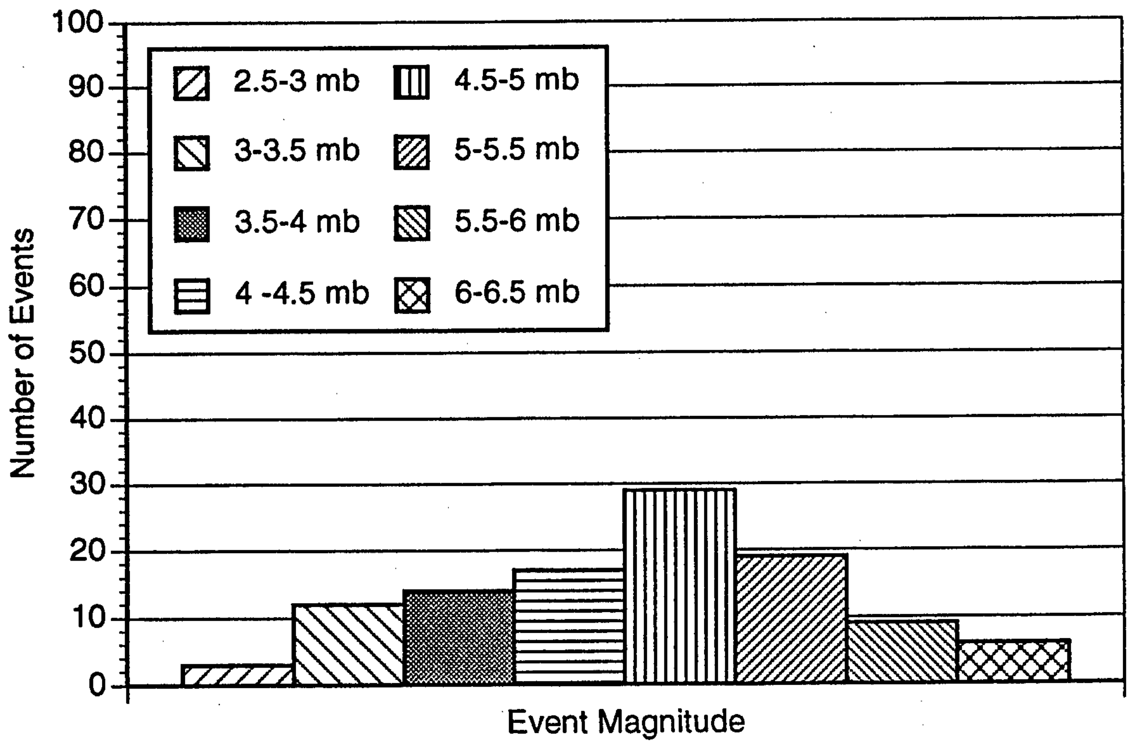

Figure 6. Distribution with respect to magnitude of observations from regional earthquakes in the western U.S. and Eurasia in the current database.

discriminant (cf. Bennett et al., 1996), assuming that L_g and regional P scale similarly with magnitude.

3. Analyses of Empirical Data

3.1 Background for L_g/P Ratios as Discriminants

The status of regional seismic discrimination was reviewed by Blandford (1981) and by Pomeroy et al. (1982). Of the 15 discriminant measures considered by Pomeroy et al., the L_g/P ratio was one of six regional observations assessed to be most promising for event identification. The original observational basis for the use of L_g/P amplitude ratios as discriminants between underground nuclear explosions and earthquakes was from studies by Willis (1963) and Willis et al. (1963). Willis found that recordings of NTS nuclear explosions and nearby earthquakes observed at a distance of 450 km showed differences in L_g/P_n, S_n/P_n, and S_n/P_g amplitude ratios, with the largest differences seen for L_g/P_n. Willis et al., using observations from a global database of explosions and earthquakes, found that nearly 80 percent of the earthquakes had larger L_g/P ratios than explosions. However, Pomeroy (1977) and Pomeroy and Nowak (1979) found conflicting evidence between observations of L_g/P for the eastern U.S. and the western areas of the former Soviet Union. While L_g/P ratios were much larger for earthquakes in the eastern U.S. than for the single nuclear explosion (viz. SALMON), a sample of explosions and earthquakes from the former Soviet Union produced roughly equal L_g and P amplitudes for both event types. Blandford (1981) was able to achieve substantial success in separating L_g/P amplitude ratios for western U.S. earthquakes and underground nuclear explosion tests by adjusting the measurements for distance differences, presumably related to attenuation. He found that L_g/P amplitude ratios were a factor of 3-5 larger for eastern and western U.S. earthquakes than for U.S. nuclear explosions when the observations were adjusted for amplitude decay to a common range of 1000 km. Murphy and Bennett (1982) looked systematically at the L_g and regional P amplitudes from a sample of NTS explosions and earthquakes within 100 km of NTS recorded at a range of about 530 km and found that the L_g/P ratios for nuclear explosions and earthquakes had statistically indistinguishable populations. However, it should be noted that the waveform data in some of these early studies is not always of highest quality and that time-domain observations frequently suffer from bandwidth limitations of the recording systems in use at the time.

Taylor et al. (1989) assessed the variety of regional discriminant measures identified by Pomeroy et al. (1982) on the basis of observations from a large sample of NTS explosions and western U.S. earthquakes recorded at the Lawrence Livermore National Laboratory (LLNL) seismic network surrounding NTS at ranges of 225 km to 400 km from the explosions. These data represent a significant improvement in quality and quantity over previous studies of regional discrimination. They found significant separation in the L_g/P_g ratios between source types but also noted considerable data scatter and overlap. Bennett et al. (1989) analyzed high-quality data recorded at a single station at somewhat larger regional distances in the western U.S. from a small sample of NTS explosions and regional earthquakes and found that the broadband L_g/P ratios were larger for the earthquakes than for the explosions. However, band-pass filter analyses of these data demonstrated conflicting results in different frequency bands, suggesting the need for refinement in these measurement techniques.

With regard to L_g/P ratios for Eurasian events, Bennett et al. (1989, 1992) investigated the ratios for Shagan River, Lop Nor, and Novaya Zemlya nuclear explosions and earthquakes in the same general region with similar epicentral distances recorded at high-quality, mainly far-regional digital stations. They found that the L_g/P ratios were frequency dependent with the ratios at frequencies of 1 Hz and lower showing similar levels for nuclear explosions and earthquakes, while above 1 Hz the ratios tended to be significantly larger for earthquakes than for explosions. Bennett et al. also found some station-dependent differences in the ratios which could be indicative of propagation effects, but comparisons of the ratios for nearly collocated explosions and earthquakes showed that much of the observed differences could be explained by source excitation differences. Baumgardt and Young (1990) and Dysart and Pulli (1990) investigated L_g/P ratios for small earthquakes and mine blasts in northern Europe and Scandinavia recorded primarily at near-regional high-quality array stations. They also found that earthquakes normally produced larger ratios than the blasts, but the implications for discrimination of nuclear explosions are not clear because we have only very limited experience comparing the excitation of L_g and regional P signals from large industrial blasts and nuclear explosions in similar source environments.

3.2 L_g/P Ratio Behavior in the Western U.S.

As noted above, the original development of regional phase spectral ratios as discriminants was based primarily on analysis of near-regional (viz. ranges less than about 800 km) signals from NTS nuclear explosions and earthquakes in the western U.S.; and these data still provide the best controlled sample for comparing the behavior of regional phases from these types of sources. Therefore, the initial phases of this project have focused on additional careful analyses of some of these data. In particular, we computed L_g/P ratios as a function of frequency using the results of band-pass filter analyses applied to the vertical-component records at the LLNL regional network stations from ten NTS underground nuclear explosions and eight nearby earthquakes. Figure 7 shows the locations of the stations and events. Because of the proximity of the explosions and earthquakes and similarity of paths, we would not expect significant differences in the L_g and regional P signals due to propagation differences; but we will analyze these effects in greater detail as the research continues. In the band-pass filter processing we have used a set of fairly broad, overlapping filter passbands (cf. Bennett et al., 1989, 1996) throughout most of the analyses. Examples of the results from application of these filters to some typical near-regional records were shown in Bennett et al. (1996) and will not be repeated here. The maximum L_g and P amplitudes were measured from the filter output in each frequency passband, and the corresponding ratios were computed and plotted as a function of filter center frequency. In the later stages of this project, we plan to investigate alternative filtering procedures as well as different measures of L_g and regional P signal strength. Because the measurements of L_g and P are from the same frequency band, we would not expect any effect from instrument response and simplified magnitude-scaling laws would indicate that L_g and P have similar frequency dependence, so that there should be little effect on their ratio from magnitude differences between events.

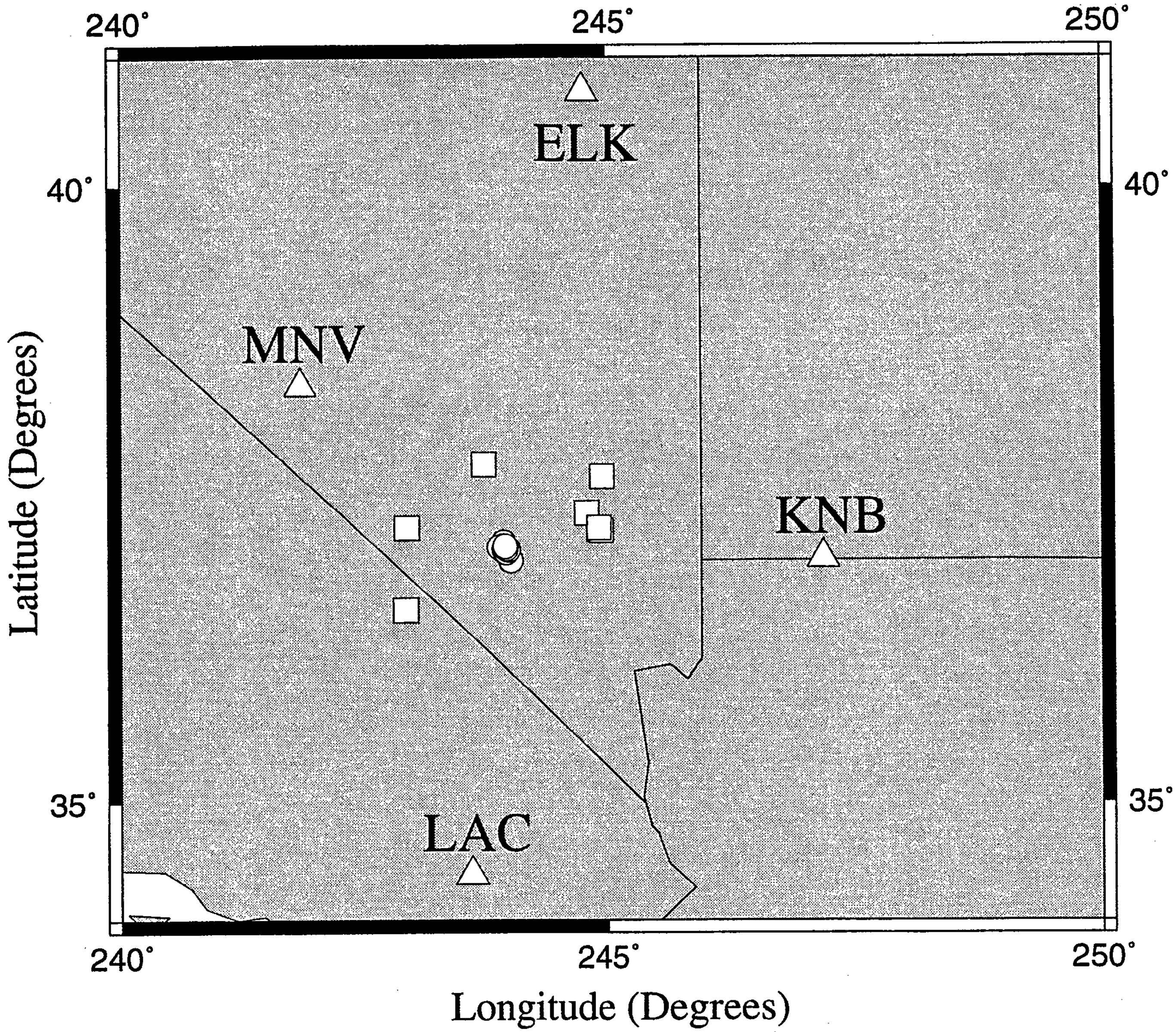

Figure 7. Map showing the locations of NTS nuclear explosions and nearby earthquakes relative to the LLNL network stations.

Figure 8 shows L_g/P ratios as a function of frequency for eight NTS nuclear explosions recorded at LLNL station KNB (R = 290 km). In general, the ratios have values between one and three at frequencies below about 1 Hz and decline toward higher frequencies. The ratios have values between about one and 0.2 at frequencies above 2 Hz, although there seems to be considerable variability between events. Figure 9 shows similar L_g/P ratios for five earthquakes recorded at KNB. In this case the ratios have values between two and five at frequencies below about 1 Hz and show only a slight decline with increasing frequency. The earthquake ratios have values between about one and five at frequencies above 2 Hz. Figure 10 shows the L_g/P spectral ratios averaged over the events for each source type at station KNB. This figure tends to make the general trends more clear; as the average L_g/P ratio is only about a factor of 1.5 larger for earthquakes at frequencies of 1 Hz and lower, but above about 3 Hz the average L_g/P ratio is about a factor of five larger for the earthquakes.

In Figure 11, we illustrate the consistency in the average L_g/P ratios between stations. The plot compares the average L_g/P ratios as a function of frequency for the NTS nuclear explosion sample recorded at each of the LLNL stations. The average ratios are surprisingly consistent varying by only about a factor of 1.5 around the average determined from all the stations and events. Trends in the slopes of the average curves are notably similar between stations; the biggest differences seem to be in the ratio levels at the individual stations.

Overall the analyses of the western U.S. data indicate that L_g/P ratios are larger for underground nuclear explosions than for earthquakes. The ratios appear to show more separation between source types at frequencies above about 2 Hz. Over the frequency band analyzed, the earthquake ratios tend to maintain values above one out to high frequencies; while the nuclear explosion ratios drop off more rapidly toward high frequencies to values well below one. One interpretation for this behavior would be that the regional P and L_g signals have similar spectral content for the earthquake source, but for the explosion source either the high frequency content of L_g is depleted or the high frequency content of the regional P is enhanced or some combination of these effects prevails. A somewhat troubling aspect of our western U.S. observations from the

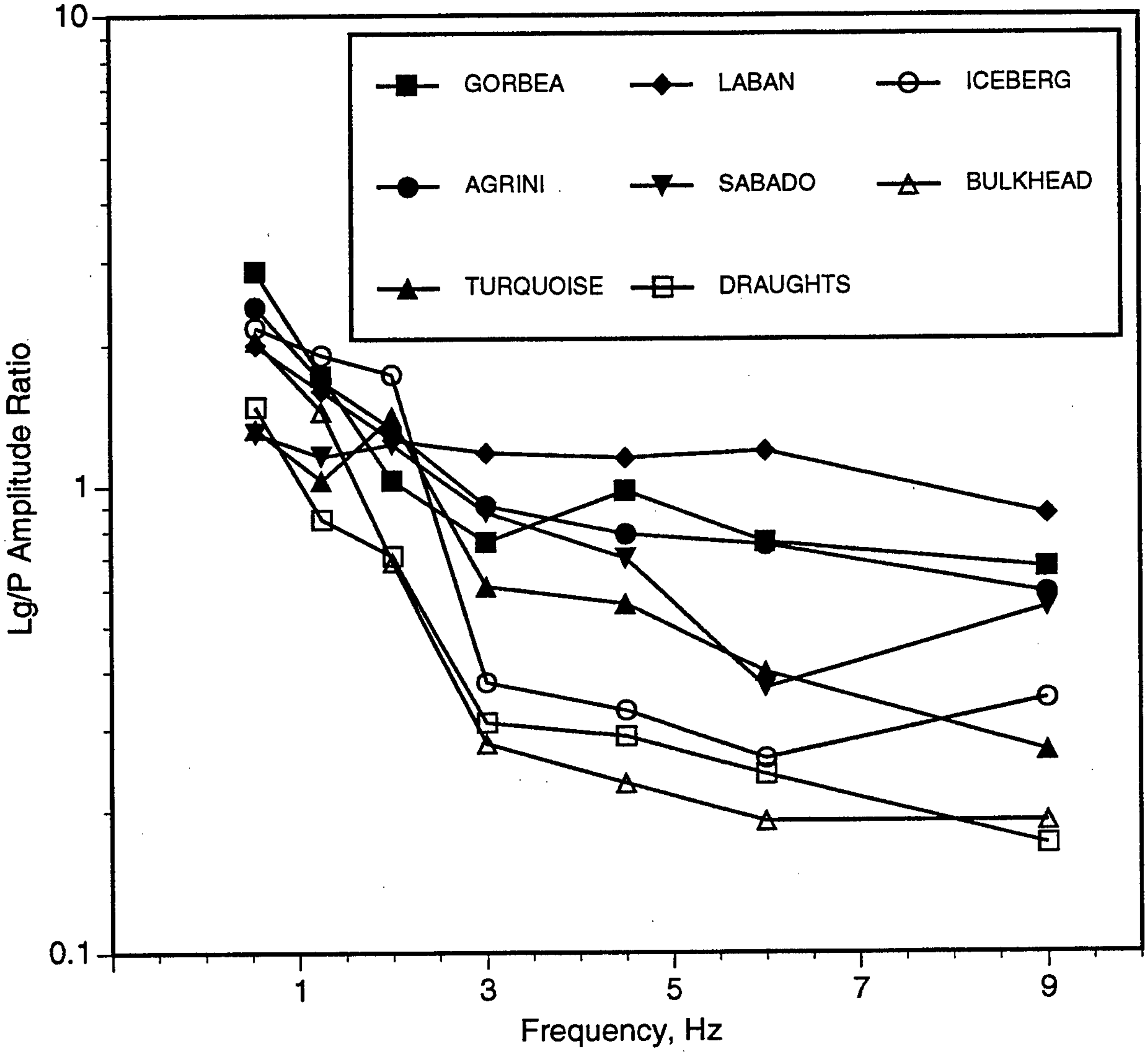

Figure 8. Lg/P amplitude ratios as a function of frequency at station KNB for NTS underground nuclear explosion tests.

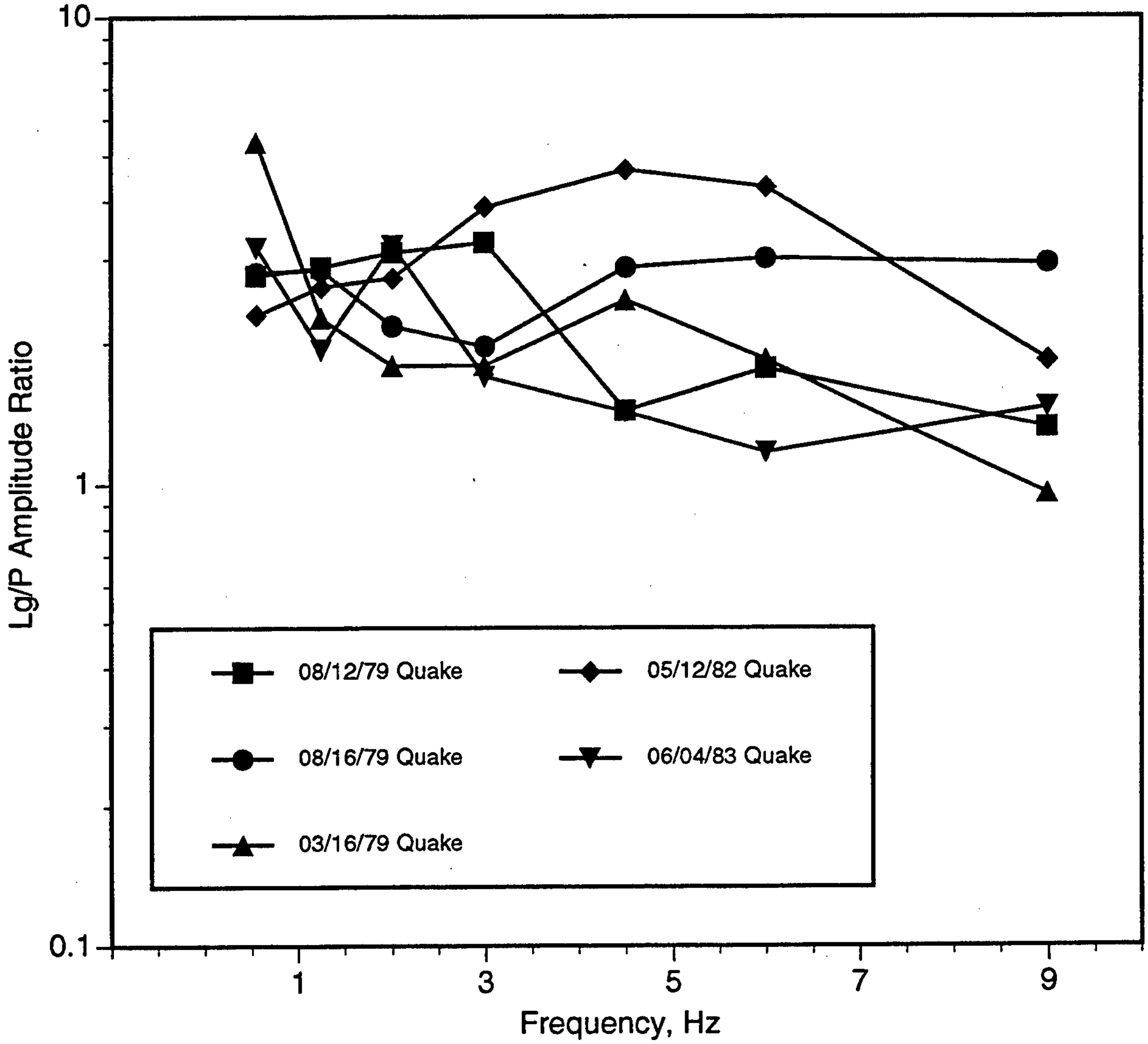

Figure 9. Lg/P amplitude ratios as a function of frequency at station KNB for a sample of earthquakes near NTS.

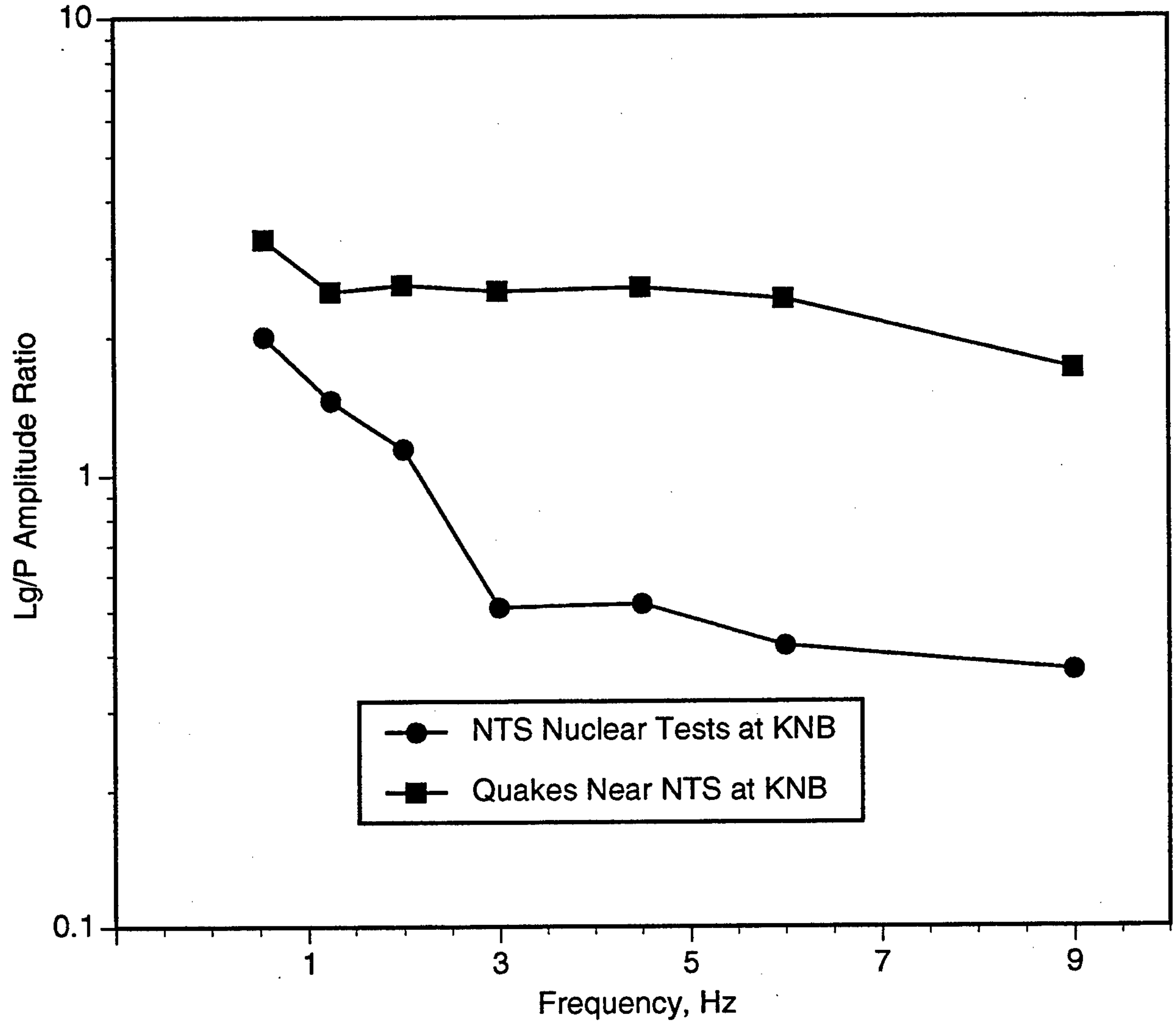

Figure 10. Comparison of average Lg/P amplitude ratios as a function of frequency at station KNB for NTS nuclear tests and nearby earthquakes.

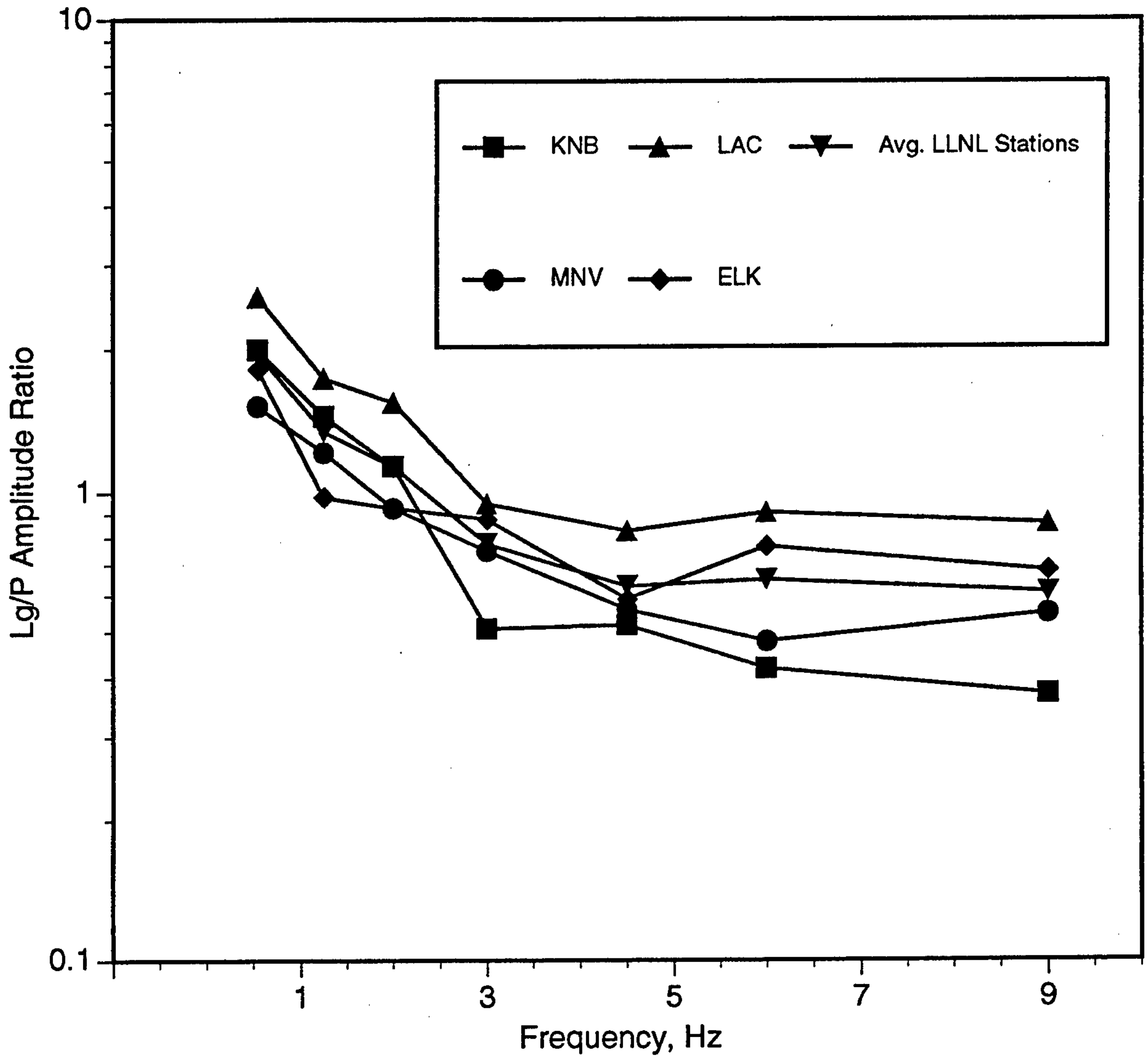

Figure 11. Comparison of average Lg/P amplitude ratios as a function of frequency from each of the LLNL network stations with overall average for ten NTS underground nuclear explosion tests.

standpoint of disciminant reliability is the relatively large scatter in the L_g/P measurements between sources at a common station. Some of the variations for the earthquakes may be attributable to source or propagation differences between events, but the variability in the explosion ratios would not appear to be related to these factors since the sources and propagation paths are nearly the same from event to event. In fact, the observation of similar average L_g/P spectral ratios at the different stations when the measurements were averaged over the available explosions seems to suggest that the path differences are relatively small contributors to the overall variability. In the latter phases of this research project, we hope to test some alternative measures of L_g and P signal strength which may provide more consistent L_g/P ratios for particular sources.

3.3 L_g/P Ratio Behavior in Eurasia

We performed the same band-pass filter analyses to determine L_g/P spectral ratios for a sample of Eurasian nuclear explosions and earthquakes. We focused our initial efforts for this region on careful analyses of the records at the CDSN station WMQ in China. For many years this station was the nearest regional station to the former Soviet test site at Shagan River, and the sample of data collected at this station from the numerous explosions provide an important link to extend regional monitoring of nuclear explosions to areas outside the western U.S. Figure 12 shows the locations of five Shagan River underground nuclear explosions and five regional earthquakes at similar distances (R = 980 km) relative to WMQ. We used the same, rather broad, overlapping band-pass filters as used in analyzing the western U.S. data and applied them to the vertical-component records at WMQ.

In Figure 13, we show the L_g/P amplitude ratios as a function of filter center frequency for each of the five explosions and five earthquakes. At frequencies of 1 Hz and below, the L_g/P ratios have values between about 1.5 and 7; and there is little distinction between the two source types. However, the L_g/P ratios for the nuclear explosions fall off very rapidly at frequencies above 2 Hz; so that the ratios are between about .05 and .15 for the nuclear explosions. In comparison, above 2 Hz the earthquake L_g/P ratios fluctuate between about 0.2 and 1.5. So, we again see similar distinctions in

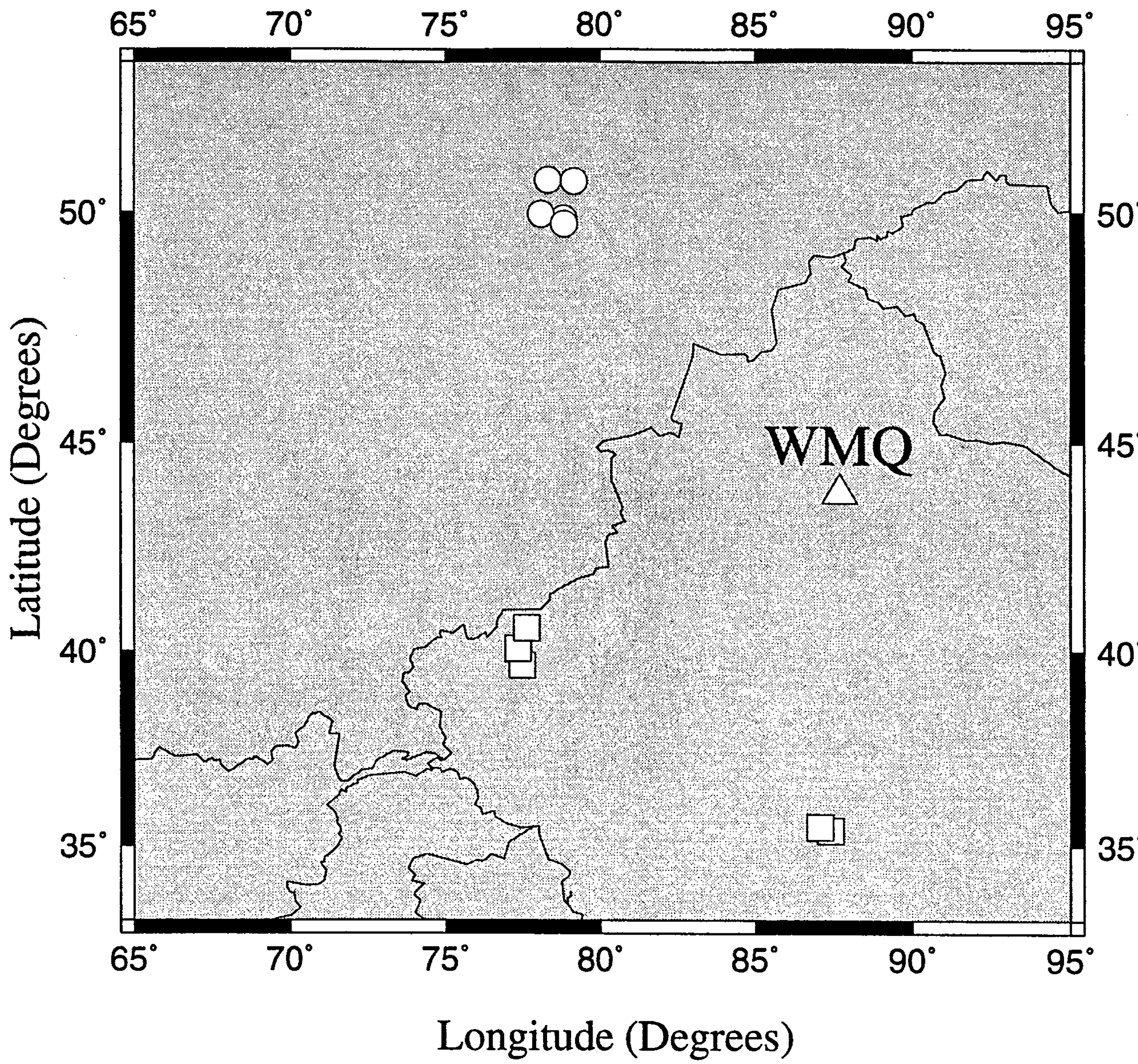

Figure 12. Map showing the locations of Soviet nuclear explosions and nearby earthquakes relative to station WMQ in China.

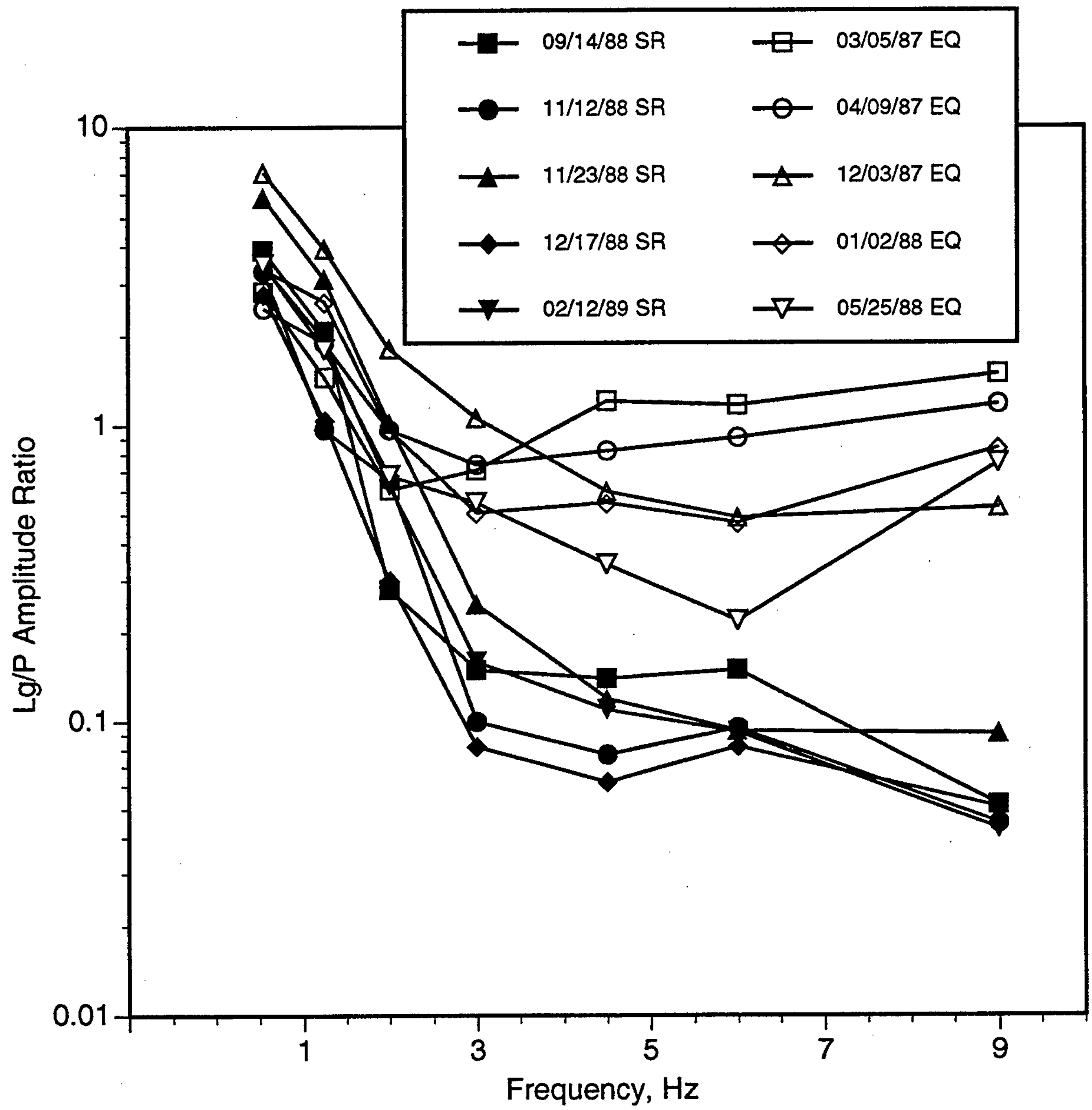

Figure 13. Lg/P amplitude ratios as a function of frequency at station WMQ for Shagan River nuclear explosions and earthquakes at similar epicentral distances.

the L_g/P ratios with higher ratios for earthquakes than explosions and larger differences at higher frequencies. With regard to consistency between events, the L_g/P ratios as a function of frequency for the nuclear explosions observed at WMQ are remarkably consistent between events, particularly with regard to the spectral shape. The variability for the explosions here is much smaller than that which we saw above in Figure 8 for the NTS explosions. The variability in the L_g/P ratios between Shagan River explosions is only about a factor of 2-3 compared to about a factor of 7 for the NTS events in Figure 8. The variability in the earthquake L_g/P ratios here is about a factor of 5, nearly the same as that seen above in Figure 9 for earthquakes in the western U.S. The largest variations for the earthquakes in both areas are at frequencies between about 4 and 6 Hz.

Figure 14 shows the average L_g/P ratios determined from the five SR explosions and from the five regional earthquakes. The average ratios are very similar for the explosions and earthquakes at frequencies below about 2 Hz, with values near one. Above 2 Hz the average earthquake L_g/P ratio remains fairly steady at a value near 0.8-1, while the average explosion L_g/P ratios fall to values from .07 to .15. So, above 2 Hz the difference between the average explosion and average earthquake L_g/P ratios at WMQ is a factor of 5 to 14.

To provide some comparisons with other Eurasian nuclear explosions, we computed L_g/P spectral ratios for five PNEs recorded at regional distances from the high-quality station at Borovoye, BRV; unfortunately no regional records from comparable earthquakes are currently available for this station. The locations of the explosions with respect to BRV are shown in Figure 15. Four of the events are at similar far-regional epicentral distances (800 km < R < 990 km) but at different azimuths around BRV, and the fifth PNE was at a near-regional distance from BRV (R = 310 km). Figure 16 shows the L_g/P ratios as a function of filter center frequency for the five PNEs. These ratios generally show more variability than was seen for the Shagan River explosions, and the trends are less clear. There does appear to be an overall decline in the ratios toward higher frequencies. However, the frequency dependence in the L_g/P ratio is quite different for the nearest PNE (viz. 08/28/73), which suggests that the consistency between events might be improved by adjusting for attenuation differences. Also, some

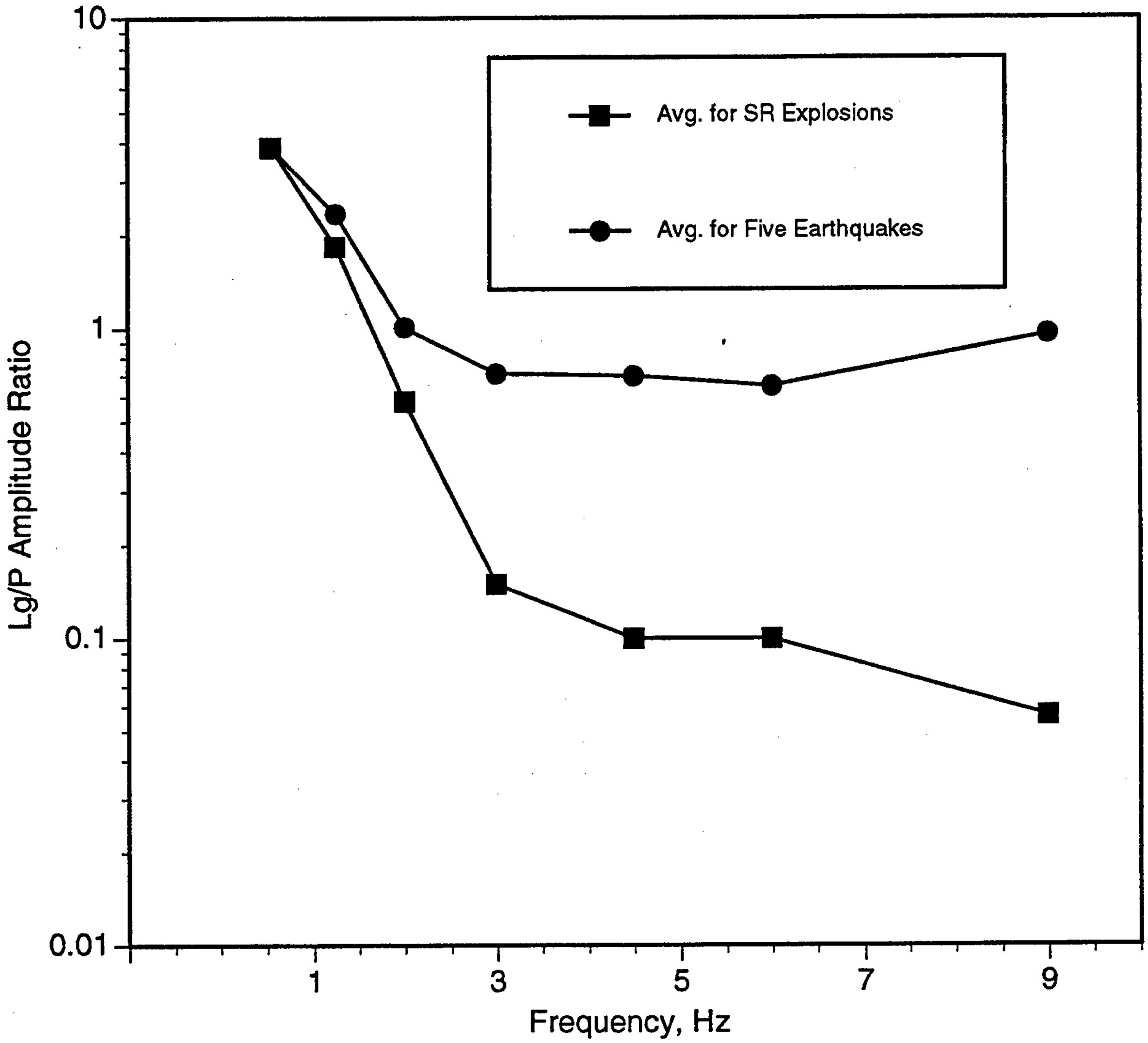

Figure 14. Comparison of average Lg/P amplitude ratios as a function of frequency at station WMQ for five Shagan River nuclear tests and five earthquakes at similar distances.

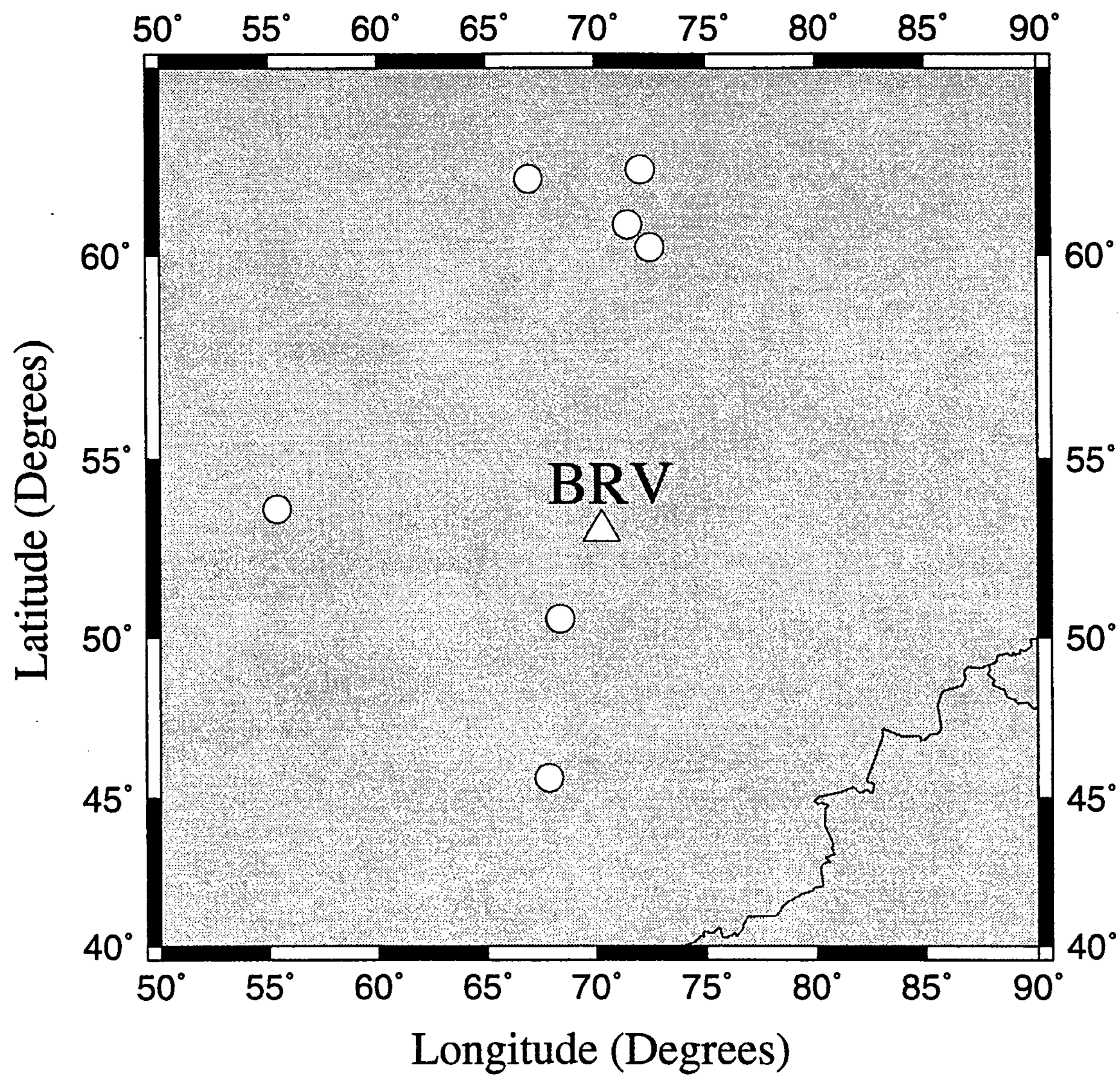

Figure 15. Map showing the locations of selected Soviet PNE explosions relative to station BRV.

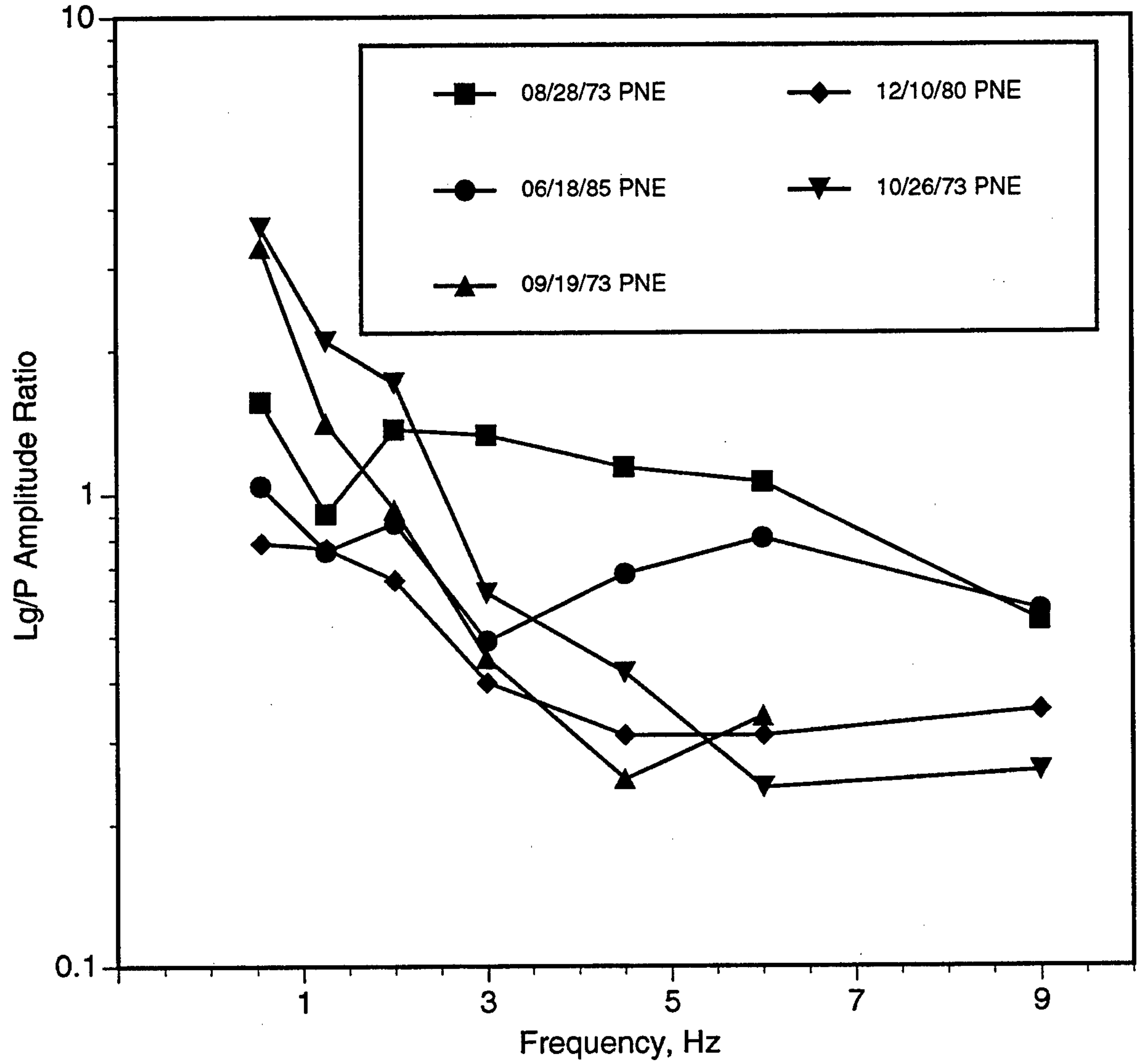

Figure 16. Lg/P amplitude ratios as a function of frequency at station BRV for five PNE tests at epicentral distances less than 1000 km.

unusual azimuthal effects have been noted for the regional signals around station BRV (cf. Murphy et al., 1996; Bennett et al., 1996) which could explain some of the differences in the spectral shapes of the L_g/P ratios, even though the epicentral distances are similar. In Figure 17, we compare the average L_g/P spectral ratios for the four PNEs at similar distances recorded at BRV with the average ratios for the five Shagan River underground nuclear tests recorded at WMQ, as shown in Figure 14. The average L_g/P ratios are fairly similar at frequencies below about 2 Hz and both show fairly rapid decline in levels above 2 Hz; however, the decline is more rapid for the Shagan River events. At frequencies from 3 to 9 Hz, the L_g/P spectral ratio levels are about a factor of four lower for the Shagan River events than for the PNEs. As noted above, the relatively high L_g/P ratios for the PNEs could be related to the anomalous azimuthal propagation effects on regional signals around station BRV. In fact, the L_g/P ratios for the PNEs at southern (viz. 09/19/73) and western (viz. 10/26/73) azimuths from BRV show more rapid fall off in the L_g/P ratios with increasing frequency and are more similar to the Shagan River event ratios. The PNEs at more northerly azimuths from BRV show a weaker P_n phase and a strong P_g phase which are different from the other records (cf. Murphy et al., 1996), and this could be affecting the L_g/P spectral ratios. We anticipate that some additional refinements in the measurement procedures and adjustments for propagation differences could reduce some of the scatter in the L_g/P ratios for the PNEs at BRV and increase their similarity to the Shagan River explosions.

3.4 Comparisons Between Regions

Finally, as part of the empirical element of this research project, we have sought to make some preliminary comparisons of the behavior of the L_g/P spectral ratios between different regions. We have made no attempt, as yet, in these comparisons to adjust for differences in observation distance or attenuation which could affect the regional phase spectra and the corresponding spectral ratios. Figure 18 shows average L_g/P ratios, determined as described above, for several different nuclear explosion samples. In general, the L_g/P ratios have average values above one at lower frequencies (below about 2 Hz) and then show a decline toward higher frequencies. It is interesting

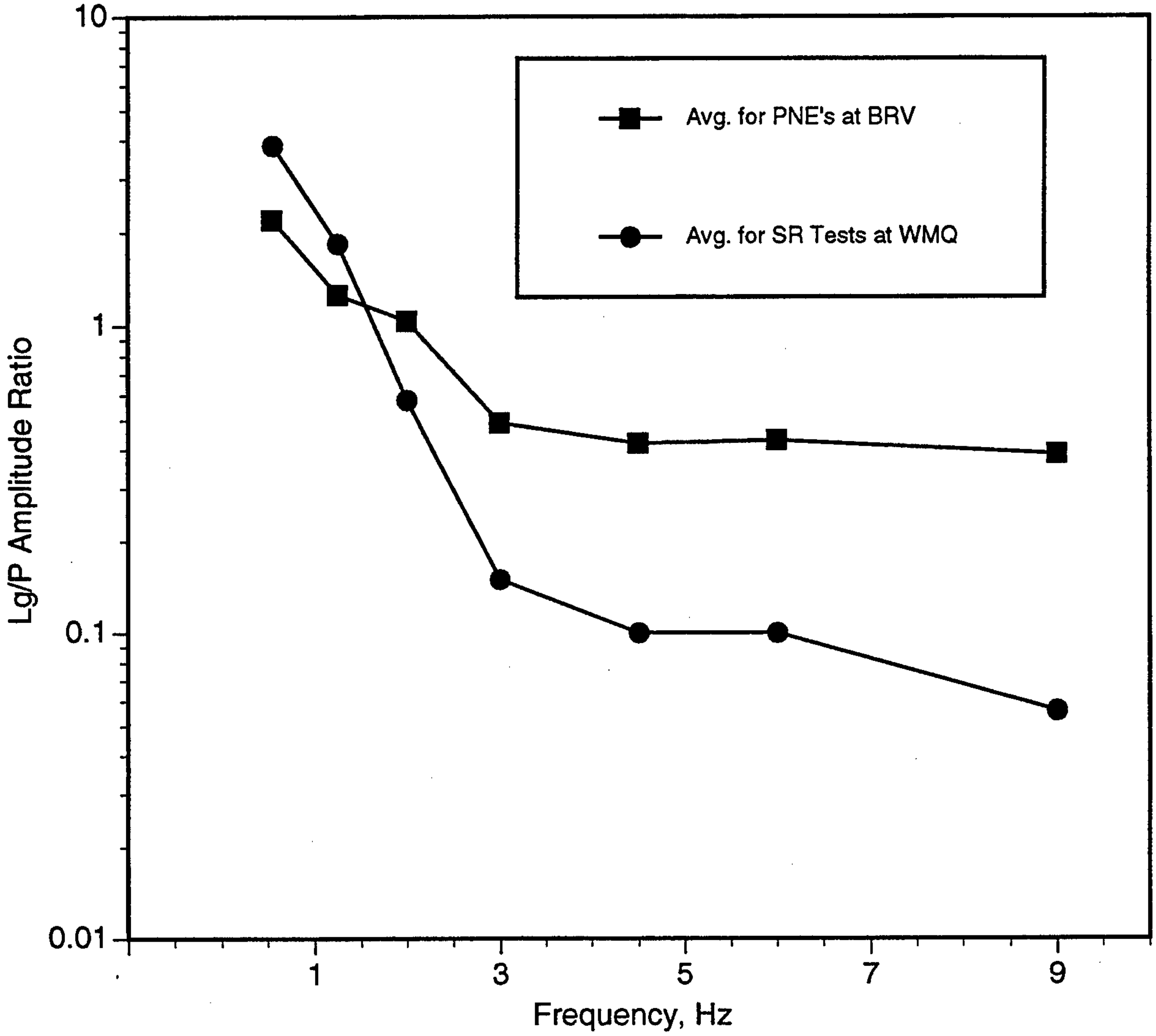

Figure 17. Comparison of average Lg/P amplitude ratios as a function of frequency for four PNE's at station BRV and five Shagan River nuclear tests at station WMQ recorded at similar epicentral distances.

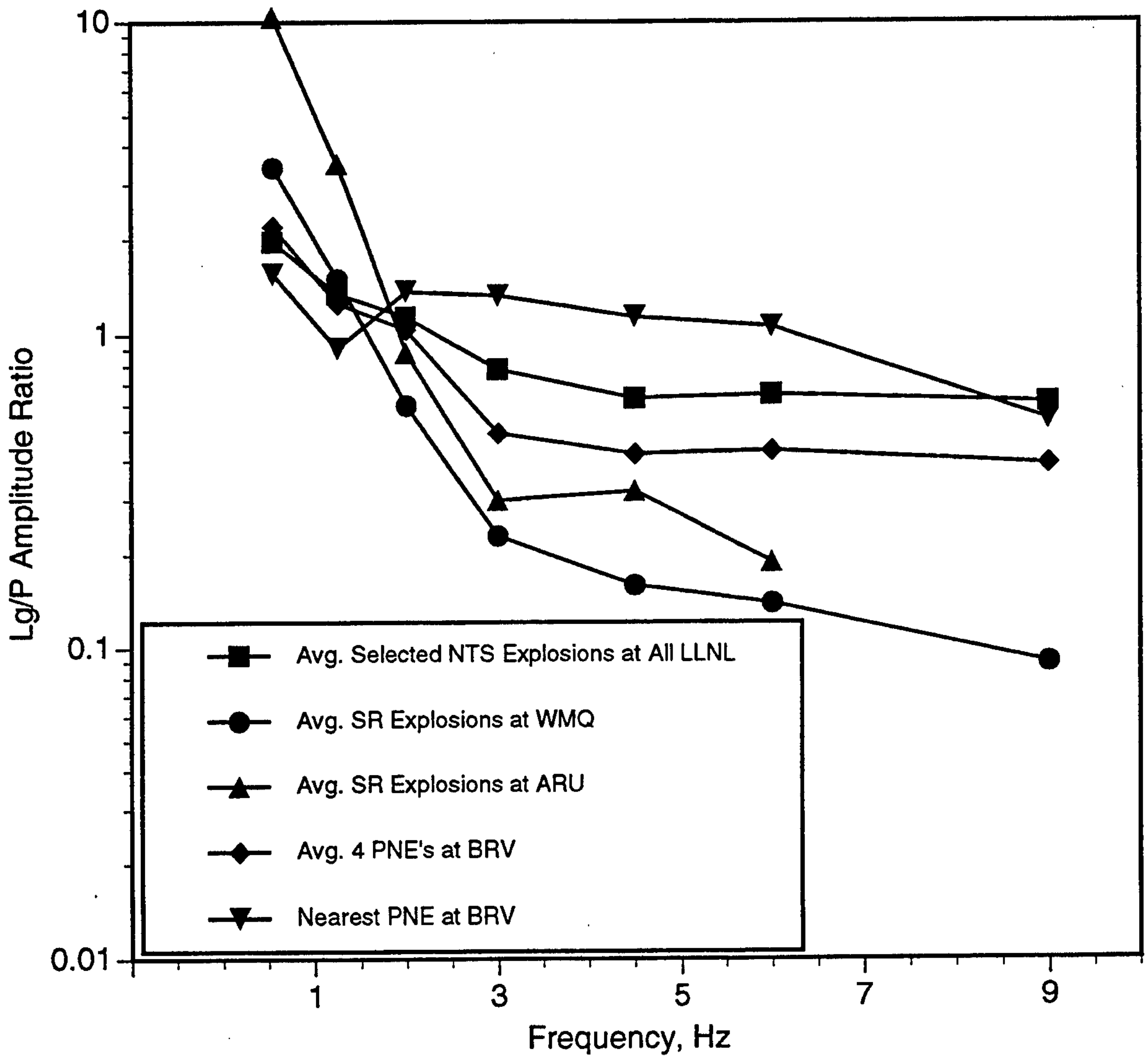

Figure 18. Comparisons of Lg/P amplitude ratios as a function of frequency for selected samples of underground nuclear explosions from several source regions.

to note some of the similarities in the L_g/P ratio spectral shapes in the figure. First, for the farther regional observations at WMQ (R = 980 km) and ARU (R = 1500 km) from Shagan River underground nuclear explosions, the L_g/P spectral ratios appear very similar. The values are well above one at low frequencies and then drop off very rapidly with increasing frequencies. There are also strong similarities in the L_g/P spectral shapes between the average for NTS explosions at all LLNL stations and the average for the four PNEs at similar distances around BRV. There the L_g/P ratios coincide at low frequencies at values just above one and then decline more slowly with increasing frequencies. The L_g/P spectral ratio for the single PNE nearest BRV has values near those of the other explosions at low frequencies, but at higher frequencies the ratios tend to be higher for this event. In general, the L_g/P ratios show sharper decline with frequency for the observations at the farther regional stations. At the nearer stations the ratios still show some decrease with frequency, and the decline seems to be somewhat greater in regions where crustal attenuation is stronger (e.g. vicinity of NTS).

Figure 19 shows average L_g/P spectral ratios for several earthquake samples. The ratios here are generally larger than those for the nuclear explosions in Figure 18. The ratios tend to be larger where the stations are closer (e.g. near-NTS earthquakes and eastern U.S. events). For the farther regional observations (e.g. earthquakes at WMQ and ARU), the L_g/P spectral ratios fall off but still tend to remain at or near one at high frequencies. Finally, we show in Figure 20 the L_g/P spectral ratios for an additional category of events important to CTBT monitoring (viz. rockbursts). Average L_g/P spectral ratios are shown for rockbursts in three different regions (viz. South Africa, Poland, and eastern U.S.) as measured at selected nearer-regional stations. The spectral shapes in Figure 20 are fairly similar and not much different from those for the earthquakes in the previous figure. The ratios tend to be the greatest at low frequencies (below about 2 Hz) with values in the range 2-5. The L_g/P values for the rockbursts show a slow decline with increasing frequency with the decrease being slightly greater for the eastern U.S. events.

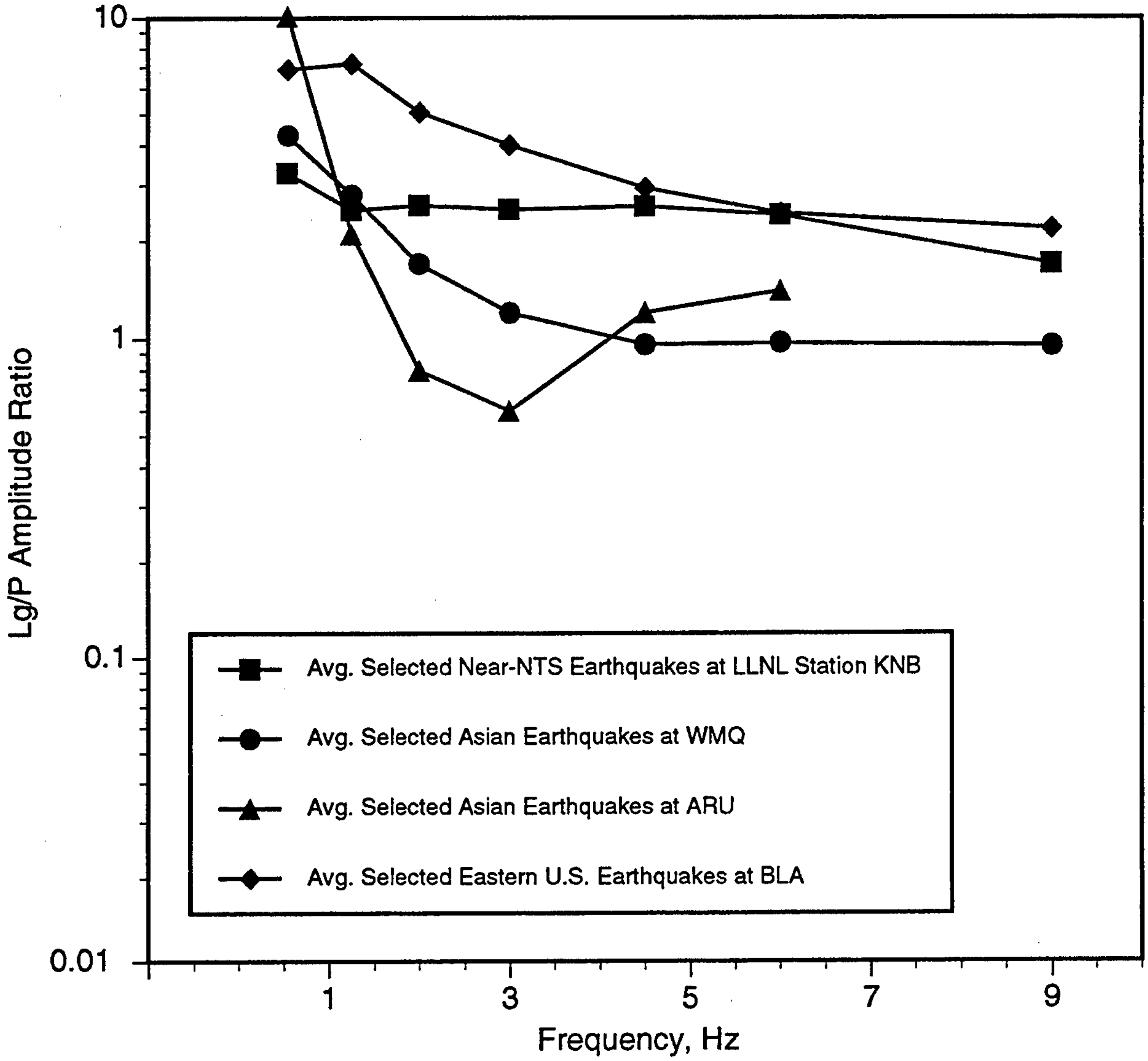

Figure 19. Comparisons of Lg/P amplitude ratios as a function of frequency for selected samples of earthquakes from several source regions.

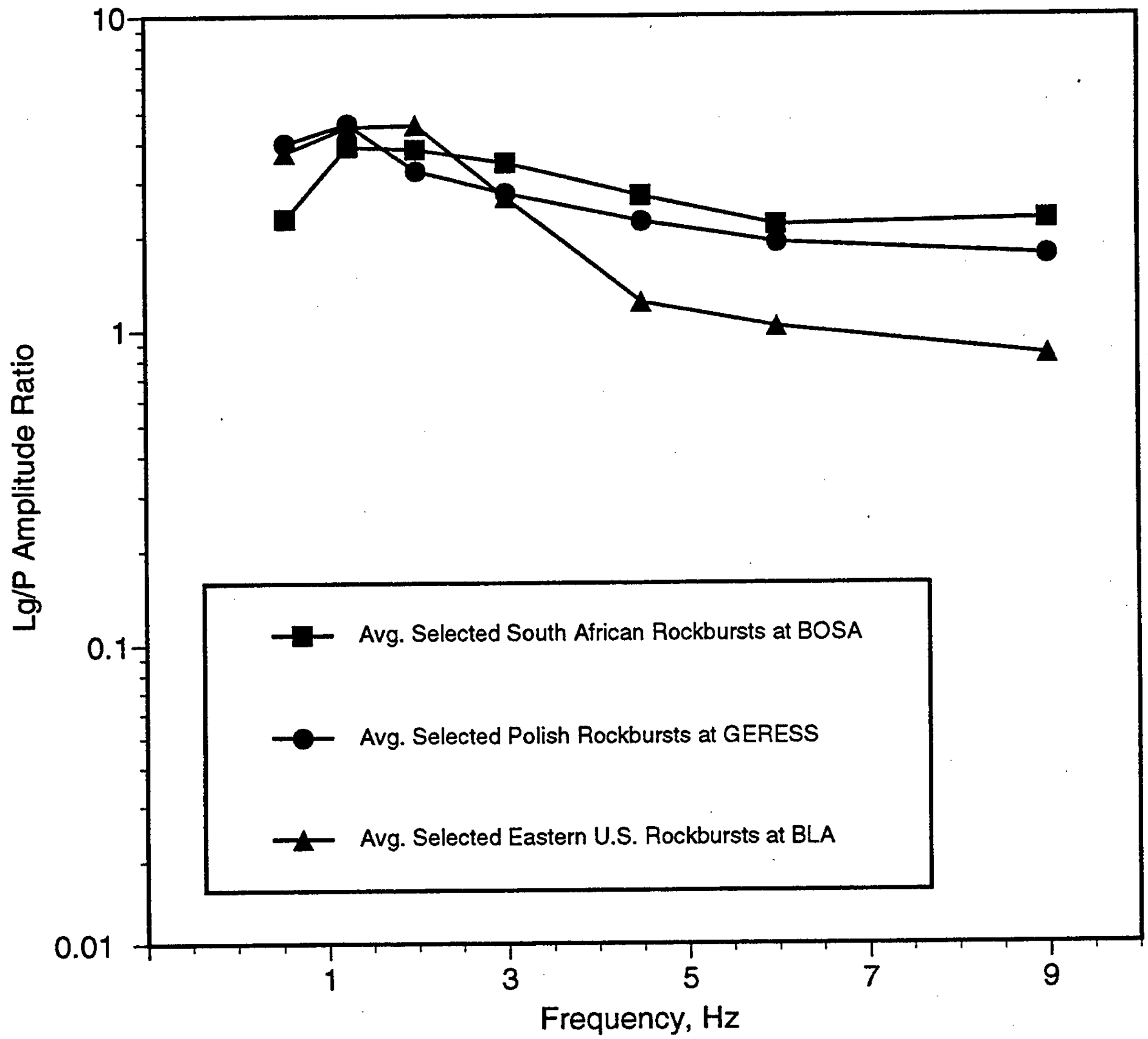

Figure 20. Comparisons of Lg/P amplitude ratios as a function of frequency for rockbursts from several mining regions.

4. Theoretical Basis for Understanding of L_g/P Ratios

4.1 Modeling Regional Behavior of L_g and P Signals

It is tacitly assumed that explosions show larger L_g/P ratios because explosions are more isotropic and more efficient radiators of P waves than of S waves. Mechanisms for the generation of regional S and L_g by explosions fall into two categories. Either they depend upon the conversion of seismic energy radiated by the isotropic source into S waves or they add non-isotropic components into the explosion source. We can list the mechanisms for L_g generation by explosions as follows:

- P→S conversion at the free surface above the isotropic explosion,
- P→S conversion at horizontal interfaces near the source,
- P→S conversion at non-horizontal interfaces and lateral heterogeneities,
- R_g→S conversion by lateral heterogeneities,
- S radiation by the spallation source near the surface above the explosion, and
- non-isotropic S radiation by deviatoric earthquake-like components in the source.

Clearly, all of these mechanisms are at work to some degree or another in any seismic source, and it may be that two or more mechanisms are responsible to a major degree for the differences that we observe in L_g/P ratios between sources. There are basically three primary observations that we would like to explain with one or more of these mechanisms. First, the consistency of the 0.5-to-1.0 Hz L_g amplitude versus explosion yield suggests that the mechanism is a stable part of the normal buried explosion source. Second, the L_g/P ratio near 1 Hz is often larger for earthquakes than for explosions; although our spectral observations from the preceding section suggest that the results at low frequencies are often mixed in some areas. Third, the explosion L_g spectra fall off faster than earthquakes with increasing frequency. The second observation leads to an L_g/P ratio discriminant near 1 Hz. The third observation leads to an L_g spectral slope (or L_g spectral ratio) discriminant and the improved discrimination capability for L_g/P ratio measurements at frequencies above 1 Hz.

In this section of the report, we describe theoretical modeling efforts focused on the effectiveness of R_g to L_g conversion as a source of the L_g signals from explosion sources. A recent investigation by Patton et al. (1995) argued that nulls in the L_g signals near 0.7 Hz from explosions at NTS could be explained by R_g excited by the spallation source and then subsequently converted from R_g to L_g. In this case, the argument presented is that the compensated linear vector dipole (CLVD) source has a null for the excitation of the fundamental Rayleigh wave near 0.7 Hz. The NTS observations indicated that the null was present for normally buried explosion shots that produced spallation, but absent for an over-buried shot that did not produce spallation. We examine in Section 4.2 the feasibility of the hypothesis that R_g-to-L_g conversion is an important source of L_g at 1 Hz. It is possible from theoretical considerations to quantify the upper bounds on the amount of L_g amplitude relative to far-field P-wave amplitude. These bounds are rigid and assume that ALL R_g energy is converted into P-SV higher modes, which arrive in the L_g window without scattering into the L_g coda or into SH higher modes. For two realistic crustal models (viz. NTS and East Kazakhstan), we have found that the upper bounds on the L_g/P ratio from the $R_g \rightarrow L_g$ mechanism are comparable to the L_g/P ratios expected from the explosion source alone generated by P→S conversion at the free surface and by P→S conversion at horizontal interfaces near the source. Since it is likely that the scattered energy will be distributed into SH as well as SV modes, the $R_g \rightarrow L_g$ scattering mechanism can only at best match these two mechanisms in effectiveness at 1 Hz. Since the $R_g \rightarrow L_g$ mechanism predicts rapidly decreasing L_g amplitudes above 1 Hz, it is even less likely that the mechanism contributes significantly to L_g above 1 Hz.

4.2 Upper Bounds on the Scattering of R_g into L_g

It has been suggested by Patton and Taylor (1995) and others (e.g. Jih and McLaughlin, 1988; Gupta et al. 1991; and Xie and Lay 1994) that scattering of short period Rayleigh waves may be a significant source of L_g from shallow explosions. In a simple layered Earth structure, pure explosion sources only excite L_g waves by conversion of compressional wave energy at interfaces such as the free surface, and the conversion of such compressional wave energy to shear-wave energy that will be trapped in the crust as L_g is inefficient. The P-wave velocity at the explosion's shallow depth of burial (200 to 1000 m) will often be close to or higher than the shear-wave velocity below the Moho (~4500 m/s); and, therefore, the explosion does not excite much P-wave energy at wavenumbers that can be converted to S-waves trapped in the crust by plane layered interfaces. The consistency of $m_b(L_g)$ as a yield estimator has led researchers to search for a robust mechanism whereby explosion generated seismic energy can be converted into short-period S waves trapped in the crust as L_g. The strength and reliability of explosion-generated short-period fundamental Rayleigh waves known as R_g led several researchers to propose the R_g-to-L_g scattering mechanism as a solution to the explosion-generated L_g problem. Attenuation for short-period R_g is strong and probably dominated by scattering from near-surface lateral heterogeneity; R_g waves at 1 Hz rarely survive to distances of 100 km.

In the following, we estimate the maximum L_g that could occur from this mechanism assuming that 1) all of the R_g scatters into P-SV L_g, and 2) seismic energy is conserved. This analysis leads to an upper bound on the L_g amplitude that can be produced by the R_g-to-L_g scattering mechanism.

The vertical displacement from the initial R_g wave u_z^0 has the form

$$u_z^0(\omega,z,r) = A_0(\omega)\exp(-ikr)E_2(k,z)/\sqrt{r} \quad (1)$$

where k is the wave number ω/c, ω is the angular frequency, z is the depth, E_2 is the Rayleigh wave vertical displacement eigenfunction which is normalized to 1 at the free surface z = 0, and A_0 is amplitude spectrum which depends on characteristics of the source and source region earth structure. The radial displacement has a similar form with E_2 replaced by the radial eigenfunction E_1. The kinetic energy T in the mode is given by

$$T_0 = \tfrac{1}{2}\omega^2 \int_0^\infty \rho(|u_z|^2 + |u_r|^2)dz = \frac{\omega^2}{2r}|A_0(\omega)|^2 I_1^0 \quad (2)$$

where I_1^0 is the energy integral on the left with the superscript indicating the fundamental mode. I_1 is the notation used by Takeuichi and Saito (1972) for this integral. In the notation of Harkrider (1964)

$$I_1^0 = \frac{1}{2cUA_R} \tag{3}$$

where U is the group velocity and A_R is Harkrider's amplitude factor.

If u_z^0 is now converted to a sum of higher modes, we have

$$u_z^{\,1} = \sum_{i=1}^{N} A_i(\omega)\exp(-ik_i r)E_2^i(k,z)/\sqrt{r} \tag{4}$$

which using the orthogonality of the modes has a total energy of

$$T_1 = \frac{\omega^2}{2r}\sum_{i=1}^{N}\left|A_i(\omega)\right|^2 I_1^i\,. \tag{5}$$

So from equations 2 and 5 and the requirement for conservation of energy we have

$$\left|A_0(\omega)\right|^2 I_1^0 = \sum_{i=1}^{N}\left|A_i(\omega)\right|^2 I_1^i\,. \tag{6}$$

Equation 6 constrains the values of A_i. Although we do not know how much energy scatters into individual modes, we can use this constraint to place some bounds on the L_g amplitude. If the amplitude of each mode is the same then

$$\left|\frac{A_i}{A_0}\right| = \sqrt{\frac{I_1^0}{\sum_{I=1}^{N} I_1^i}} = \frac{1}{\sqrt{N}}\sqrt{\frac{I_1^0}{I_1^i}} \tag{7}$$

and if the modes add incoherently, then

$$\left|\frac{u_z^1}{u_z^0}\right|_{even} \approx \sqrt{\frac{I_1^0}{I_1^i}} \tag{8}$$

The maximum L_g amplitude will occur if all of the R_g energy transfers to the single L_g mode with the minimum energy. In that case we have

$$\left|\frac{u_z^1}{u_z^0}\right|_{\max} \approx \sqrt{\frac{I_1^0}{I_1^{\min}}}\,. \tag{9}$$

If the energy is equally partitioned among all of the higher modes, then we can expect

$$\left|\frac{u_z^1}{u_z^0}\right|_{equipartition} \approx \sqrt{\left[\frac{I_1^0}{I_1^i}\right]}. \qquad (10)$$

Equations 8-10 provide some reasonable upper bounds on the scattering of R_g into L_g. It is interesting to note that Eq. 8 and 10 do not explicitly include the number of modes but only averages of the modal energy integrals, (I_1^i) and their inverse $(1/I_1^i)$.

Figure 21 shows the values of the energy integrals, I_1^i, calculated at a frequency of 1 hz for the first 10 modes in three earth structures: a Gutenberg Earth model and models for the Nevada Test Site (NTS) and the former Soviet East Kazakh test site (Stevens, 1986). Note that for mode numbers greater than 3 the energy integrals are nearly constant for each model. The energy in these modes is distributed throughout the crust.

The relative amplitudes of Eq. 8-10 are listed in Table 1. For the energy equipartition scattering model, the results are fairly consistent, approximately 15% for each of the three earth models. Scattering ratios vary from about 6% to 50% for the other scattering models. The equipartition model is attractive in that it predicts that the L_g amplitudes will be approximately the same fraction of R_g amplitude for all three models.

The numbers in Table 1 represent upper bounds of spectral amplitude of L_g relative to the predicted spectral amplitude of the fundamental mode not attenuated by scattering. For example, to use these results to compute upper bounds on spectral L_g/P ratios we must first compute the predicted spectral ratio of R_g/P. Furthermore, if we wish to use these results to compute upper bounds on the time domain amplitudes we must make some assumptions about the time duration of the L_g signal. For example we might assume that the L_g energy is distributed over a group velocity interval from 3.6 to 2.0 km/s and invoke random vibration theory to estimate peak amplitudes. In practice however, the $R_g \rightarrow L_g$ conversion will probably be more spread out in time and contribute to the L_g coda as well as the traditional L_g group velocity window. Another mechanism that may contribute to lower upper bounds of L_g energy that could be converted from R_g is the conversion of P-SV R_g and P-SV L_g to SH L_g. It is reasonable to believe that R_g scattering will contribute to the transverse modes of L_g as well as the P-SV modes; and,

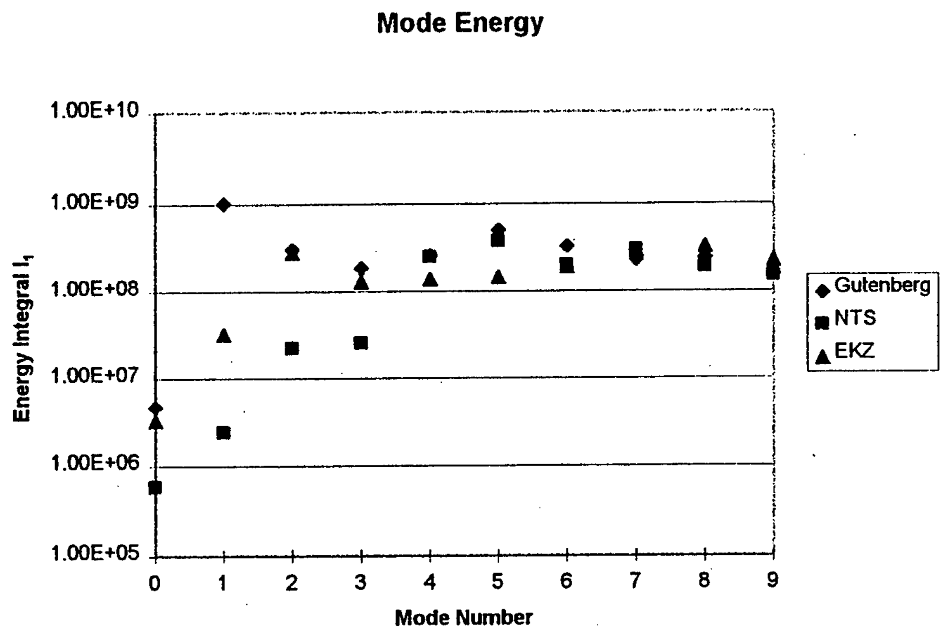

Figure 21. Energy in each mode in three different earth models.

Model	Gutenberg	NTS	EKZ
Equal amplitude	0.114	0.059	0.129
Equipartition	0.131	0.185	0.162
Maximum	0.172	0.494	0.318

Table 1. Scattering ratios for three types of distribution among higher modes: equal amplitude, equipartition of energy, and maximum amplitude in a single mode.

Model	Gutenberg	NTS	EKZ
L_g/P from explosion source	1.7	5.0	3.0
L_g/P R_g->L_g scattered from explosion source	11	6.2	8.1

Table 2. L_g/P amplitude spectral ratios at 500 km for three models from an explosion point source at a depth of 500 m. In each case, the R_g->L_g generated L_g spectral energy is comparable to the L_g energy directly excited by the explosion source.

therefore, we can expect perhaps only 50% of the R_g energy may be available for the P-SV modes of L_g. Gupta and Blandford (1983) suggested just this equipartition of energy may be taking place between the P-SV and SH modes of L_g and suggested this as a mechanism for the short-period transverse motion from explosions observed at regional distances.

As an example of the use of these bounds on P-SV L_g from R_g scattering, we estimated the spectral amplitude ratios of L_g/P for the three models at a distance of 500 km at 1 Hz. Figure 22 shows a synthetic vertical component velocity seismogram bandpassed between 0.75 and 1.25 Hz for an explosion point source (10^{14} Nt-m) at a depth of 500 m. The shear-wave attenuation of the EKZ model has been increased so as to make the intrinsic attenuation of the fundamental mode Rayleigh wave (R_g) insignificant. From this seismogram the spectral amplitudes of P, L_g, and R_g were measured and tabulated. The spectral amplitude ratio bound can be estimated from $L_g/P = (R_g/P) * (R_g \rightarrow L_g/R_g)$, where (R_g/P) is the ratio of R_g to P measured from the seismogram in Figure 22 and $(R_g \rightarrow L_g / R_g)$ is the scattering ratio from Table 1. For the EKZ model we get a ratio of about 8 at 1 Hz. For comparison, the L_g/P ratio for the point source explosion is 3. If 100% of the explosion R_g is converted to P-SV L_g, the L_g spectral amplitude would nearly double. The results for the three models are summarized in Table 2 assuming the equipartition of modal energy. The L_g generated by R_g to L_g scattering would range from 120% to 640% percent of the direct L_g. If we consider a CLVD source as suggested by Patton and Taylor (1995) then the $R_g \rightarrow L_g$ scattered L_g spectral amplitudes are reduced by 25% for the Gutenberg model and nearly the same for the NTS and EKZ models.

In summary, we have investigated upper bounds on the mechanism of R_g-to-L_g conversion using simple modal energy integrals assuming only 1) all R_g energy is converted to P-SV higher modes and 2) all seismic energy is conserved. These upper bounds may be lowered if we consider the additional conversion of R_g and P-SV modes to SH modes, or P and S energy that leaks out of the crustal wave guide, or intrinsic attenuation of R_g. Three Earth structures considered all predict approximately the same relative amplitude between the near-field R_g and the far-field L_g.

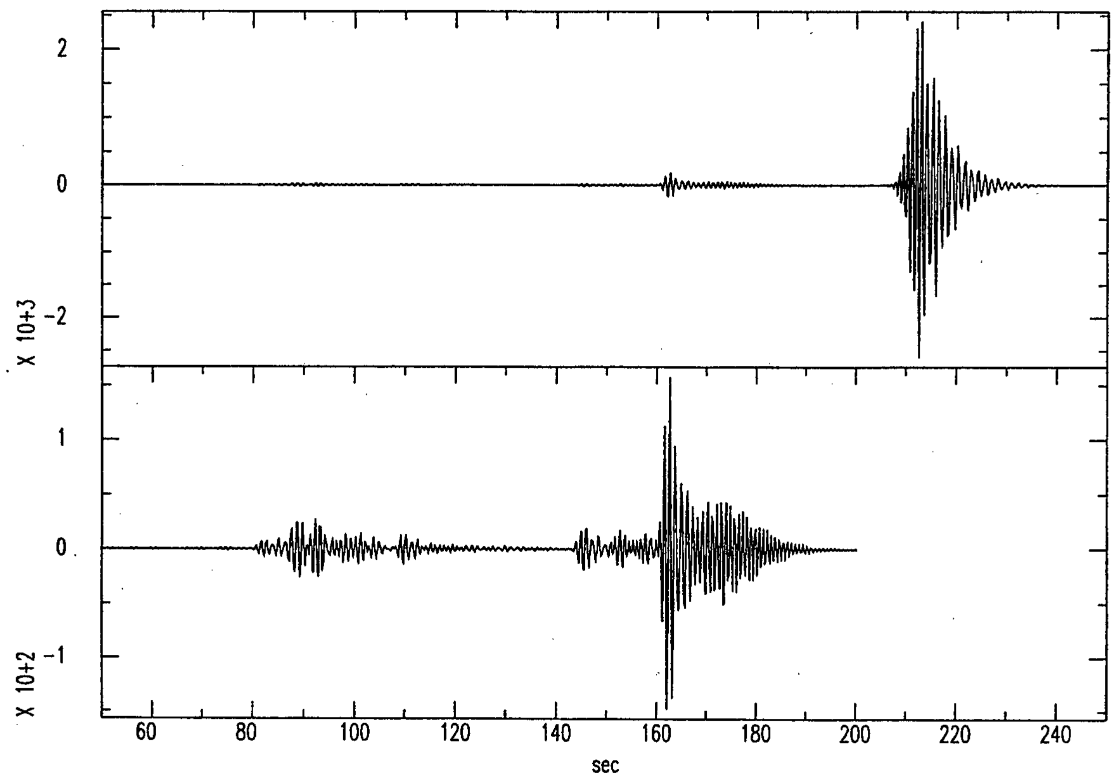

Figure 22. Vertical component synthetic seismogram (0.75-1.25Hz) at a distance of 500km from a 10^{14} Nt-m point explosion source at a depth of 500m in the EKZ model. The upper panel shows the complete synthetic seismogram. The lower panel shows the P and Lg waveforms at a higher magnification. There is 50 times more spectral amplitude in the Rg than the P wave; however, if all of the Rg seismic energy is converted to incoherent higher mode energy, the expected Lg spectral amplitude would only be 270% larger than the direct Lg.

5. Summary and Plans

5.1 Summary of Main Findings

This research program has involved two principal elements: (1) an empirical element to determine the characteristic behavior of L_g/P amplitude ratios for the various seismic source types in different tectonic environments, and (2) a theoretical element to analyze the influences of the factors in the different source mechanisms and propagation environments on the L_g/P ratios and to provide the physical basis for the observed behavior. During the initial phase of this research the empirical element has focused on careful review of the behavior of the L_g/P ratios and their dependence on frequency for good-quality recordings of regional signals from nuclear explosions in several different tectonic regions, earthquakes at similar regional distances and tectonic environments, and selected alternative source types (viz. rockbursts) in several different regions. The theoretical studies so far have focused primarily on the effectiveness of various mechanisms for generation of L_g by explosive sources.

In our review of the available regional seismic data, we have collected a large representative database of regional seismic signals from nuclear tests, earthquakes, non-nuclear blasts and rockbursts in a variety of propagation environments. As described in Section 3, we have determined the behavior of L_g/P amplitude ratios and their dependence on frequency from many of these events and have found that they tend to be consistent with experience indicating larger L_g/P ratios for earthquakes and rockbursts than for nuclear explosions. Furthermore, the spectral studies show that the differences in the ratios between the source types tend to be greater at higher frequencies (above about 2 Hz). One negative aspect of the observations with regard to discrimination reliability is that, although the average L_g/P spectral ratios show some clear differences between source types, there seemed to be considerable scatter in the ratios for some of the individual events. In some cases this seemed to be related to possible propagation differences (e.g. for the PNE explosions at different azimuths around station BRV), but we also found some unusual scatter in the ratios for events of similar source type and nearly common propagation paths (e.g. for some of the nuclear tests recorded by the

LLNL network stations). It is hoped that refinements which are being developed for the spectral estimation procedures and regional phase windowing will improve the consistency of the measurements.

In Section 4, we presented theoretical upper bounds on L_g/P ratios from $R_g \rightarrow L_g$ scattering for realistic NTS and East Kazakhstan crustal models. We compared these upper bounds at 1 Hz to the expected L_g/P ratios from an explosion source in a layered-earth model where the L_g signal is produced by conversion of P waves at the free surface and other horizontal layers. We found that the hard upper bounds from the scattering model are comparable to the explosion L_g from the alternative model. Since several mechanisms are certainly at work to reduce $R_g \rightarrow L_g$ scattered energy below the projected upper bounds, we find it likely that the $R_g \rightarrow L_g$ scattering mechanism is a relatively minor contributing mechanism to L_g at 1 Hz for nuclear explosions. Furthermore, since the $R_g \rightarrow L_g$ mechanism theoretically predicts a rapid decline in L_g amplitude as a function of increasing frequency, it is very unlikely that the mechanism contributes to L_g at frequencies above 1 Hz. This decrease in L_g generated from R_g with increasing frequency results because the R_g generation by the shallow explosion source declines exponentially at higher frequencies. While this might explain the empirical observation of the rapid decline in L_g/P ratios from explosion sources with increasing frequency, it is likely that some of the other mechanisms for L_g or S generation by the explosion could also be controlling the L_g signal strength in this frequency range. We hope to obtain additional insight into these alternative mechanisms in the continuing stages of this research program.

5.2 Plans for Future Work

In the empirical element of this research, we will continue to refine the observational techniques for measuring L_g/P ratios. We have been looking at alternative spectral measurements of the regional signals and methods for averaging amplitudes over group velocity windows corresponding to the L_g and regional P for the different propagation regions. We also will be looking more closely at the effects of propagation and attenuation on the regional P and L_g phases in the different regions and attempting to define appropriate corrections to the ratio measurements for such propagation effects. These results will then be related to the theoretical behavior expected for the different source types in the different propagation environments. We also intend to look at additional data from more recent events of various source types at several of the seismic stations (e.g. IDC network) which are currently important for monitoring regional events in selected source regions

For the theoretical element of the research program, we will continue over the remainder of the program with our examination of the mechanisms for L_g production from explosion sources and L_g propagation in general. We expect to refine the $R_g \rightarrow L_g$ scattering model and produce frequency-dependent upper bounds on L_g/P ratios. We have concluded three-dimensional finite difference calculations of regional propagation in crustal models with and without randomized structure. We are in the process of analyzing these calculations and will conduct several more during this year. These calculations examine the propagation of P_g and L_g in a three-dimensional crustal waveguide. These calculations will help us address the problem of $P \rightarrow L_g$ scattering near 1 Hz and the character of L_g mode-mode conversion. We have been collecting various crustal models for computation of a suite of synthetic layered-earth Green's functions. These models will be used to examine the variability of L_g/P ratios expected from various sources due to crustal variability. The hypothesis that layering in the crust can be used as a proxy for lateral heterogeneity will be examined using this suite of models.

6. References

Baumgardt, D. R., and G. B. Young (1990). "Regional Seismic Waveform Discriminants and Case-Based Event Identification Using Regional Arrays," Bull. Seism. Soc. Am., 80, pp. 1874 - 1892.

Bennett, T. J., and J. R. Murphy (1986). "Analysis of Seismic Discrimination Capabilities Using Regional Data from Western United States Events," Bull. Seism. Soc. Am., 76, pp. 1069 -1086.

Bennett, T. J., B. W. Barker, K. L. McLaughlin, and J. R. Murphy (1989). "Regional Discrimination of Quarry Blasts, Earthquakes and Underground Nuclear Explosions," GL-TR-89-0114, ADA223148.

Bennett, T. J., A. K. Campanella, J. F. Scheimer, and J. R. Murphy (1992). "Demonstration of Regional Discrimination of Eurasian Seismic Events Using Observations at Soviet IRIS and CDSN Stations," PL-TR-92-2090, ADA253275.

Bennett, T. J., M. E. Marshall, B. W. Barker, and J. R. Murphy (1996). "Investigations of Regional Phase Spectral Ratios: Transportability and Measurement Algorithms," PL-TR-96-2283.

Blandford, R. (1981). "Seismic Discrimination Problems at Regional Distances," in Identification of Seismic Source - Earthquake or Underground Explosion, D. Reidel Publishing Co., pp. 695-740.

Dysart, P. S., and J. J. Pulli (1990). "Regional Seismic Event Classification at the NORESS Array: Seismological Measurements and the Use of Trained Neural Networks," Bull. Seism. Soc. Am., 80, pp. 1910 - 1933.

Gupta, I. N. and R. R. Blandford (1983). "A Mechanism for Generation of Short-Period Transverse Motion from Explosions," Bull. Seism. Soc. Am., 73, pp. 571 - 592.

Gupta, I. N., T. W. McElfresh, and R. A. Wagner (1991). "Near-Source Scattering of Rayleigh to P in Teleseismic Arrivals from Pahute Mesa NTS Shots," in Explosion Source Phenomenology, AGU Monograph 65, pp. 151 - 159.

Harkrider, D. G. (1964). "Surface Waves in Multilayered Elastic Media, I. Rayleigh and Love Waves from Buried Sources in a Multilayered Elastic Half-Space," Bull. Seism. Soc. Am., 54, pp. 627 - 679.

Jih, R.-S., and K. L. McLaughlin (1988). "Investigation of Explosion Generated SV Lg Waves in 2-D Heterogeneous Crustal Models by Finite-Difference Method," AFGL-TR-88-0025, ADA213586..

Murphy, J. R., and T. J. Bennett (1982). "A Discrimination Analysis of Short-Period Regional Seismic Data Recorded at Tonto Forest Observatory," Bull. Seism. Soc. Am., 72, pp. 1351 - 1366.

Murphy, J. R., D. D. Sultanov, B. W. Barker, I. O. Kitov, and M. E. Marshall (1996). "Regional Seismic Detection Analyses of Selected Soviet Peaceful Nuclear Explosions," SSS-DFR-96-15503, PL-TR-96-2206.

Patton, H. J. and S. R. Taylor (1995). "Analysis of Lg Spectral Ratios from NTS Explosions: Implications for the Source Mechanisms of Spall and the Generation of Lg Waves," Bull. Seism. Soc. Am., 85, pp. 220 - 236.

Pomeroy, P. W. (1977). "Aspects of Seismic Wave Propagation in Eastern North America - A Preliminary Report," Rondout Associates Report.

Pomeroy, P. W., and T. A. Nowak (1979). "An Investigation of Seismic Wave Propagation in Western USSR," Rondout Associates Semi-Annual Technical Report No. 2.

Pomeroy, P. W., W. J. Best, and T. V. McEvilly (1982). "Test Ban Treaty Verification with Regional Data - A Review," Bull. Seism. Soc. Am., 72, pp. S89 - S129.

Stevens, J. L. (1986), "Estimation of Scalar Moments from Explosion-Generated Surface Waves," Bull. Seism. Soc. Am., v. 76, pp. 123 - 151.

Takeuchi, H, and M. Saito (1972). "Seismic Surface Waves," in Methods in Computational Physics, Vol. 11, ed. B. A. Bolt, Academic Press, New York, pp. 217 - 295.

Taylor, S. R., M. D. Denny, E. S. Vergino, and R. E. Glaser (1989). "Regional Discrimination Between NTS Explosions and Western U. S. Earthquakes," Bull. Seism. Soc. Am., 78, pp. 1142 - 1176.

Willis, D. E. (1963). "Comparison of Seismic Waves Generated by Different Types of Sources," Bull. Seism. Soc. Am., 53, pp. 965 - 978.

Willis, D. E., J. DeNoyer, and J. T. Wilson (1963). "Differentiation of Earthquakes and Underground Nuclear Explosions on the Basis of Amplitude Characteristics," Bull. Seism. Soc. Am., 53, pp. 979 - 987.

Xie, X.-B., T. Lay (1994). "The Excitation of Lg Waves by Explosions: A Finite-Difference Investigation," Bull. Seism. Soc. Am., 84, pp. 324 - 342.

THOMAS AHRENS
SEISMOLOGICAL LABORATORY 252-21
CALIFORNIA INST. OF TECHNOLOGY
PASADENA, CA 91125

AIR FORCE RESEARCH LABORATORY
ATTN: VSOE
29 RANDOLPH ROAD
HANSCOM AFB, MA 01731-3010
(2 COPIES)

AIR FORCE RESEARCH LABORATORY
ATTN: RESEARCH LIBRARY/TL
5 WRIGHT STREET
HANSCOM AFB, MA 01731-3004

AIR FORCE RESEARCH LABORATORY
ATTN: AFRL/SUL
3550 ABERDEEN AVE SE
KIRTLAND AFB, NM 87117-5776
(2 COPIES)

RALPH ALEWINE
NTPO
1901 N. MOORE STREET, SUITE 609
ARLINGTON, VA 22209

MUAWIA BARAZANGI
INSTOC
3126 SNEE HALL
CORNELL UNIVERSITY
ITHACA, NY 14853

T.G. BARKER
MAXWELL TECHNOLOGIES
8888 BALBOA AVE.
SAN DIEGO, CA 92123-1506

DOUGLAS BAUMGARDT
ENSCO INC.
5400 PORT ROYAL ROAD
SPRINGFIELD, VA 22151

THERON J. BENNETT
MAXWELL TECHNOLOGIES
11800 SUNRISE VALLEY DRIVE, STE 1212
RESTON, VA 22091

WILLIAM BENSON
NAS/COS
ROOM HA372
2001 WISCONSIN AVE. NW
WASHINGTON DC 20007

JONATHAN BERGER
UNIVERSITY OF CA, SAN DIEGO
SCRIPPS INST. OF OCEANOGRAPHY
IGPP, 0225
9500 GILMAN DRIVE
LA JOLLA, CA 92093-0225

ROBERT BLANDFORD
AFTAC
1300 N. 17TH STREET
SUITE 1450
ARLINGTON, VA 22209-2308

LESLIE A. CASEY
DEPT. OF ENERGY/NN-20
1000 INDEPENDENCE AVE. SW
WASHINGTON DC 20585-0420

CENTER FOR MONITORING RESEARCH
ATTN: LIBRARIAN
1300 N. 17th STREET, SUITE 1450
ARLINGTON, VA 22209

ANTON DAINTY
HQ DSWA/PMA
6801 TELEGRAPH ROAD
ALEXANDRIA, VA 22310-3398

CATHERINE DE GROOT-HEDLIN
UNIV. OF CALIFORNIA, SAN DIEGO
INST. OF GEOP. & PLANETARY PHYSICS
8604 LA JOLLA SHORES DRIVE
SAN DIEGO, CA 92093

DTIC
8725 JOHN J. KINGMAN ROAD
FT BELVOIR, VA 22060-6218 (2 COPIES)

DIANE DOSER
DEPT OF GEOLOGICAL SCIENCES
THE UNIVERSITY OF TEXAS AT EL PASO
EL PASO, TX 79968

MARK D. FISK
MISSION RESEARCH CORPORATION
735 STATE STREET
P.O. DRAWER 719
SANTA BARBARA, CA 93102-0719

LORI GRANT
MULTIMAX, INC.
311C FOREST AVE. SUITE 3
PACIFIC GROVE, CA 93950

HENRY GRAY
SMU STATISTICS DEPARTMENT
P.O. BOX 750302
DALLAS, TX 75275-0302

I. N. GUPTA
MULTIMAX, INC.
1441 MCCORMICK DRIVE
LARGO, MD 20774

DAVID HARKRIDER
BOSTON COLLEGE
INSTITUTE FOR SPACE RESEARCH
140 COMMONWEALTH AVENUE
CHESTNUT HILL, MA 02167

THOMAS HEARN
NEW MEXICO STATE UNIVERSITY
DEPARTMENT OF PHYSICS
LAS CRUCES, NM 88003

MICHAEL HEDLIN
UNIV. OF CALIFORNIA, SAN DIEGO
SCRIPPS INST. OF OCEANOGRAPHY
IGPP, 0225
9500 GILMAN DRIVE
LA JOLLA, CA 92093-0225

DONALD HELMBERGER
CALIFORNIA INST. OF TECHNOLOGY
DIV. OF GEOL. & PLANETARY SCIENCES
SEISMOLOGICAL LABORATORY
PASADENA, CA 91125

EUGENE HERRIN
SOUTHERN METHODIST UNIVERSITY
DEPARTMENT OF GEOLOGICAL
SCIENCES
DALLAS, TX 75275-0395

ROBERT HERRMANN
ST. LOUIS UNIVERSITY
DEPT OF EARTH & ATMOS. SCIENCES
3507 LACLEDE AVENUE
ST. LOUIS, MO 63103

VINDELL HSU
HQ/AFTAC/TTR
1030 S. HIGHWAY A1A
PATRICK AFB, FL 32925-3002

RONG-SONG JIH
HQ DSWA/PMA
6801 TELEGRAPH ROAD
ALEXANDRIA, VA 22310-3398

THOMAS JORDAN
MASS. INST. OF TECHNOLOGY
BLDG 54-918
77 MASSACHUSETTS AVENUE
CAMBRIDGE, MA 02139

LAWRENCE LIVERMORE NAT'L LAB
ATTN: TECHNICAL STAFF (PLS ROUTE)
PO BOX 808, MS L-175
LIVERMORE, CA 94551

LAWRENCE LIVERMORE NAT'L LAB
ATTN: TECHNICAL STAFF (PLS ROUTE)
PO BOX 808, MS L-208
LIVERMORE, CA 94551

LAWRENCE LIVERMORE NAT'L LAB
ATTN: TECHNICAL STAFF (PLS ROUTE)
PO BOX 808, MS L-202
LIVERMORE, CA 94551

LAWRENCE LIVERMORE NAT'L LAB
ATTN: TECHNICAL STAFF (PLS ROUTE)
PO BOX 808, MS L-195
LIVERMORE, CA 94551

LAWRENCE LIVERMORE NAT'L LAB
ATTN: TECHNICAL STAFF (PLS ROUTE)
PO BOX 808, MS L-205
LIVERMORE, CA 94551

LAWRENCE LIVERMORE NAT'L LAB
ATTN: TECHNICAL STAFF (PLS ROUTE)
PO BOX 808, MS L-200
LIVERMORE, CA 94551

LAWRENCE LIVERMORE NAT'L LAB
ATTN: TECHNICAL STAFF (PLS ROUTE)
PO BOX 808, MS L-221
LIVERMORE, CA 94551

THORNE LAY
UNIV. OF CALIFORNIA, SANTA CRUZ
EARTH SCIENCES DEPARTMENT
EARTH & MARINE SCIENCE BUILDING
SANTA CRUZ, CA 95064

ANATOLI L. LEVSHIN
DEPARTMENT OF PHYSICS
UNIVERSITY OF COLORADO
CAMPUS BOX 390
BOULDER, CO 80309-0309

JAMES LEWKOWICZ
WESTON GEOPHYSICAL CORP.
325 WEST MAIN STREET
NORTHBORO, MA 01532

LOS ALAMOS NATIONAL LABORATORY
ATTN: TECHNICAL STAFF (PLS ROUTE)
PO BOX 1663, MS F659
LOS ALAMOS, NM 87545

LOS ALAMOS NATIONAL LABORATORY
ATTN: TECHNICAL STAFF (PLS ROUTE)
PO BOX 1663, MS F665
LOS ALAMOS, NM 87545

LOS ALAMOS NATIONAL LABORATORY
ATTN: TECHNICAL STAFF (PLS ROUTE)
PO BOX 1663, MS C335
LOS ALAMOS, NM 87545

GARY MCCARTOR
SOUTHERN METHODIST UNIVERSITY
DEPARTMENT OF PHYSICS
DALLAS, TX 75275-0395

KEITH MCLAUGHLIN
CENTER FOR MONITORING RESEARCH
SAIC
1300 N. 17TH STREET, SUITE 1450
ARLINGTON, VA 22209

BRIAN MITCHELL
DEPT OF EARTH & ATMOS. SCIENCES
ST. LOUIS UNIVERSITY
3507 LACLEDE AVENUE
ST. LOUIS, MO 63103

RICHARD MORROW
USACDA/IVI
320 21ST STREET, N.W.
WASHINGTON DC 20451

JOHN MURPHY
MAXWELL TECHNOLOGIES
11800 SUNRISE VALLEY DRIVE, STE 1212
RESTON, VA 22091

JAMES NI
NEW MEXICO STATE UNIVERSITY
DEPARTMENT OF PHYSICS
LAS CRUCES, NM 88003

ROBERT NORTH
CENTER FOR MONITORING RESEARCH
1300 N. 17th STREET, SUITE 1450
ARLINGTON, VA 22209

OFFICE OF THE SECRETARY OF DEFENSE
DDR&E
WASHINGTON DC 20330

JOHN ORCUTT
INST. OF GEOPH. & PLANETARY PHYSICS
UNIV.OF CALIFORNIA, SAN DIEGO
LA JOLLA, CA 92093

PACIFIC NORTHWEST NAT'L LAB
ATTN: TECHNICAL STAFF (PLS ROUTE)
PO BOX 999, MS K6-48
RICHLAND, WA 99352

PACIFIC NORTHWEST NAT'L LAB
ATTN: TECHNICAL STAFF (PLS ROUTE)
PO BOX 999, MS K6-40
RICHLAND, WA 99352

PACIFIC NORTHWEST NAT'L LAB
ATTN: TECHNICAL STAFF (PLS ROUTE)
PO BOX 999, MS K6-84
RICHLAND, WA 99352

PACIFIC NORTHWEST NAT'L LAB
ATTN: TECHNICAL STAFF (PLS ROUTE)
PO BOX 999, MS K5-12
RICHLAND, WA 99352

FRANK PILOTTE
HQ AFTAC/TT
1030 S. HIGHWAY A1A
PATRICK AFB, FL 32925-3002

KEITH PRIESTLEY
DEPARTMENT OF EARTH SCIENCES
UNIVERSITY OF CAMBRIDGE
MADINGLEY RISE, MADINGLEY ROAD
CAMBRIDGE, CB3 OEZ UK

JAY PULLI
BBN SYSTEMS AND TECHNOLOGIES, INC.
1300 NORTH 17TH STREET
ROSSLYN, VA 22209

DELAINE REITER
AFRL/VSOE (SENCOM)
29 RANDOLPH ROAD
HANSCOM AFB, MA 01731-3010

PAUL RICHARDS
COLUMBIA UNIVERSITY
LAMONT-DOHERTY EARTH OBSERV.
PALISADES, NY 10964

MICHAEL RITZWOLLER
DEPARTMENT OF PHYSICS
UNIVERSITY OF COLORADO
CAMPUS BOX 390
BOULDER, CO 80309-0309

DAVID RUSSELL
HQ AFTAC/TTR
1030 SOUTH HIGHWAY A1A
PATRICK AFB, FL 32925-3002

CHANDAN SAIKIA
WOODWARD-CLYDE FED. SERVICES
566 EL DORADO ST., SUITE 100
PASADENA, CA 91101-2560

SANDIA NATIONAL LABORATORY
ATTN: TECHNICAL STAFF (PLS ROUTE)
DEPT. 5704
MS 0979, PO BOX 5800
ALBUQUERQUE, NM 87185-0979

SANDIA NATIONAL LABORATORY
ATTN: TECHNICAL STAFF (PLS ROUTE)
DEPT. 9311
MS 1159, PO BOX 5800
ALBUQUERQUE, NM 87185-1159

SANDIA NATIONAL LABORATORY
ATTN: TECHNICAL STAFF (PLS ROUTE)
DEPT. 5704
MS 0655, PO BOX 5800
ALBUQUERQUE, NM 87185-0655

SANDIA NATIONAL LABORATORY
ATTN: TECHNICAL STAFF (PLS ROUTE)
DEPT. 5736
MS 0655, PO BOX 5800
ALBUQUERQUE, NM 87185-0655

THOMAS SERENO, JR.
SAIC
10260 CAMPUS POINT DRIVE
SAN DIEGO, CA 92121

AVI SHAPIRA
SEISMOLOGY DIVISION
IPRG
P.O.B. 2286
NOLON 58122 ISRAEL

ROBERT SHUMWAY
410 MRAK HALL
DIVISION OF STATISTICS
UNIVERSITY OF CALIFORNIA
DAVIS, CA 95616-8671

MATTHEW SIBOL
ENSCO, INC.
445 PINEDA CT.
MELBOURNE, FL 32940

DAVID SIMPSON
IRIS
1200 NEW YORK AVE., NW
SUITE 800
WASHINGTON DC 20005

JEFFRY STEVENS
MAXWELL TECHNOLOGIES
8888 BALBOA AVE.
SAN DIEGO, CA 92123-1506

BRIAN SULLIVAN
BOSTON COLLEGE
INSITUTE FOR SPACE RESEARCH
140 COMMONWEALTH AVENUE
CHESTNUT HILL, MA 02167

TACTEC
BATTELLE MEMORIAL INSTITUTE
505 KING AVENUE
COLUMBUS, OH 43201 (FINAL REPORT)

NAFI TOKSOZ
EARTH RESOURCES LABORATORY, M.I.T.
42 CARLTON STREET, E34-440
CAMBRIDGE, MA 02142

LAWRENCE TURNBULL
ACIS
DCI/ACIS
WASHINGTON DC 20505

GREG VAN DER VINK
IRIS
1200 NEW YORK AVE., NW
SUITE 800
WASHINGTON DC 20005

FRANK VERNON
UNIV.OF CALIFORNIA, SAN DIEGO
SCRIPPS INST. OF OCEANOGRAPHY
IGPP, 0225
9500 GILMAN DRIVE
LA JOLLA, CA 92093-0225

TERRY WALLACE
UNIVERSITY OF ARIZONA
DEPARTMENT OF GEOSCIENCES
BUILDING #77
TUCSON, AZ 85721

JILL WARREN
LOS ALAMOS NATIONAL LABORATORY
GROUP NIS-8
P.O. BOX 1663
LOS ALAMOS, NM 87545 (5 COPIES)

DANIEL WEILL
NSF
EAR-785
4201 WILSON BLVD., ROOM 785
ARLINGTON, VA 22230

RU SHAN WU
UNIV. OF CALIFORNIA SANTA CRUZ
EARTH SCIENCES DEPT.
1156 HIGH STREET
SANTA CRUZ, CA 95064

JIAKANG XIE
COLUMBIA UNIVERSITY
LAMONT DOHERTY EARTH OBSERV.
ROUTE 9W
PALISADES, NY 10964

JAMES E. ZOLLWEG
BOISE STATE UNIVERSITY
GEOSCIENCES DEPT.
1910 UNIVERSITY DRIVE
BOISE, ID 83725